Controls on Modern Erosion and the Development of the Pearl River Drainage in the late Paleogene

Chang Liu[1], Peter Clift[1,2], Andrew Carter[3], Philipp Böning[4], Zhaochu Hu[5], Zhen Sun[6] and Katharina Pahnke[4]

1- Department of Geology and Geophysics, Louisiana State University, Baton Rouge 70803, USA
2- School of Geography Science, Nanjing Normal University, Nanjing 210023, China
3- Department of Earth and Planetary Sciences, Birkbeck College, University of London, London WC1E 7HX, UK
4- Max Planck Research Group for Marine Isotope Geochemistry, Institute of Chemistry and Biology of the Marine Environment, University of Oldenburg, PO Box 2503, D-26111, Germany
5- State Key Laboratory of Geological Processes and Mineral Resources, China University of Geosciences, Wuhan, 430074, China
6- Key Laboratory of Marginal Sea Geology, South China Sea Institute of Oceanology, Chinese Academy of Sciences, 164 Xingangxi Road, Guangzhou 510301, China

Abstract

The Pearl River and its tributaries drains large areas of southern China and has been the primary source of sediment to the northern continental margin of the South China Sea since its opening. In this study we use a combination of bulk sediment geochemistry, Nd and Sr isotope geochemistry, and single grain zircon U-Pb dating to understand the source of sediment in the modern drainage. We also performed zircon U-Pb dating on Eocene sedimentary rocks sampled by International Ocean Discovery Program (IODP) Expedition

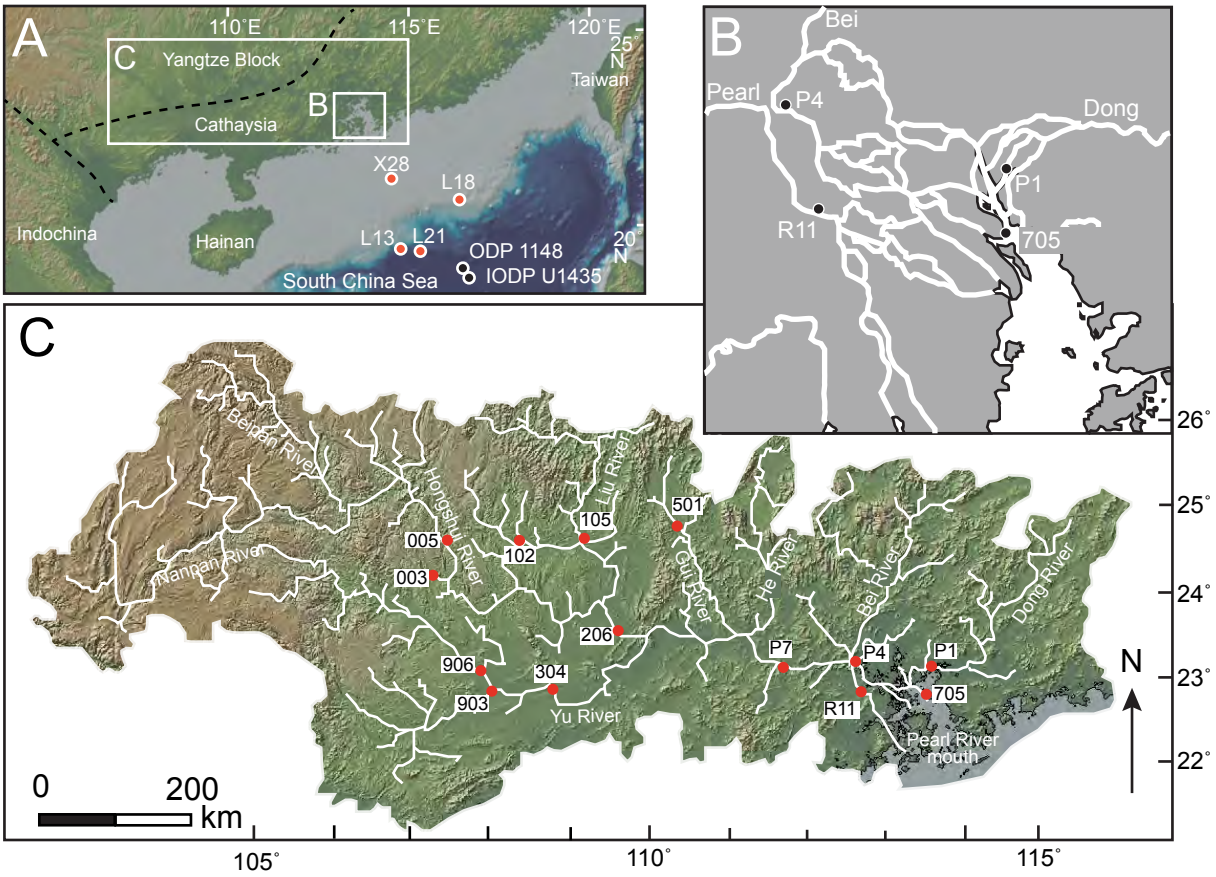

Figure 1
Liu et al

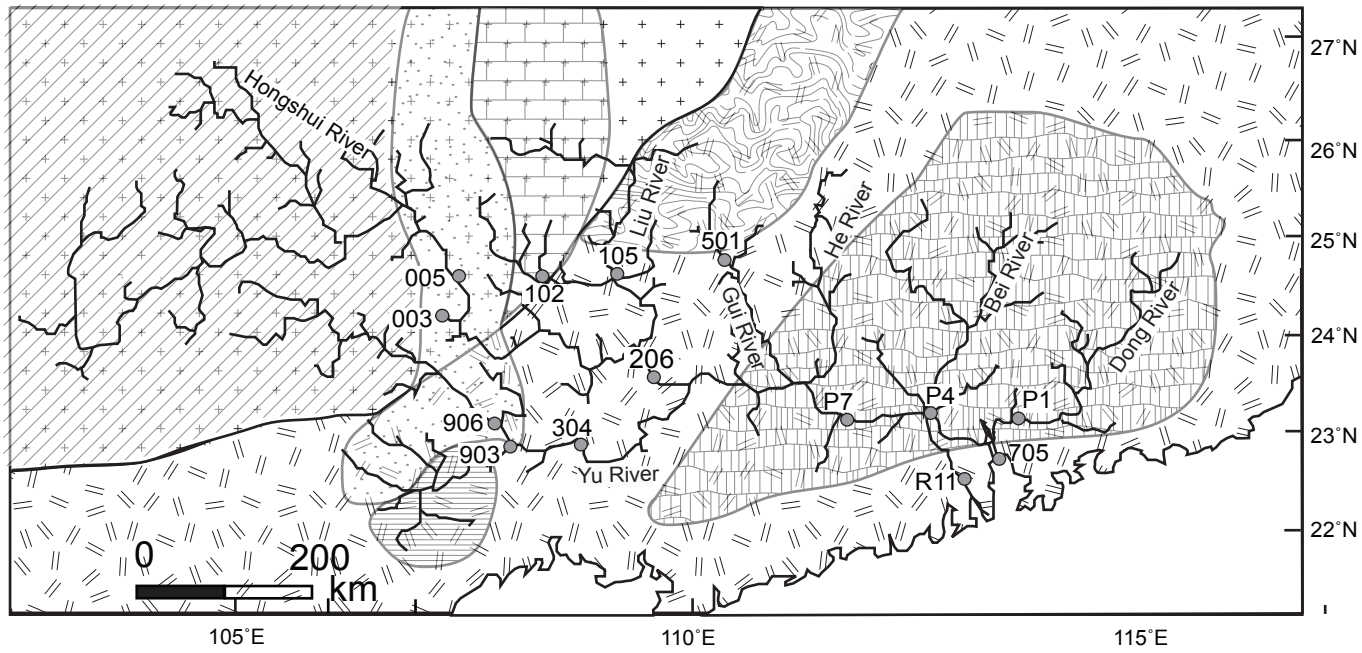

Yangtze Craton

Cathaysia

~100 Ma - Cretaceous arc influence

~250 Ma - Indosinian influence

~400 Ma - Caledonian influence

~800 Ma - Yangtze Craton influence

~1000 Ma - Cathaysia influence

~1800 Ma - Luliangian influence

Figure 2
Liu et al

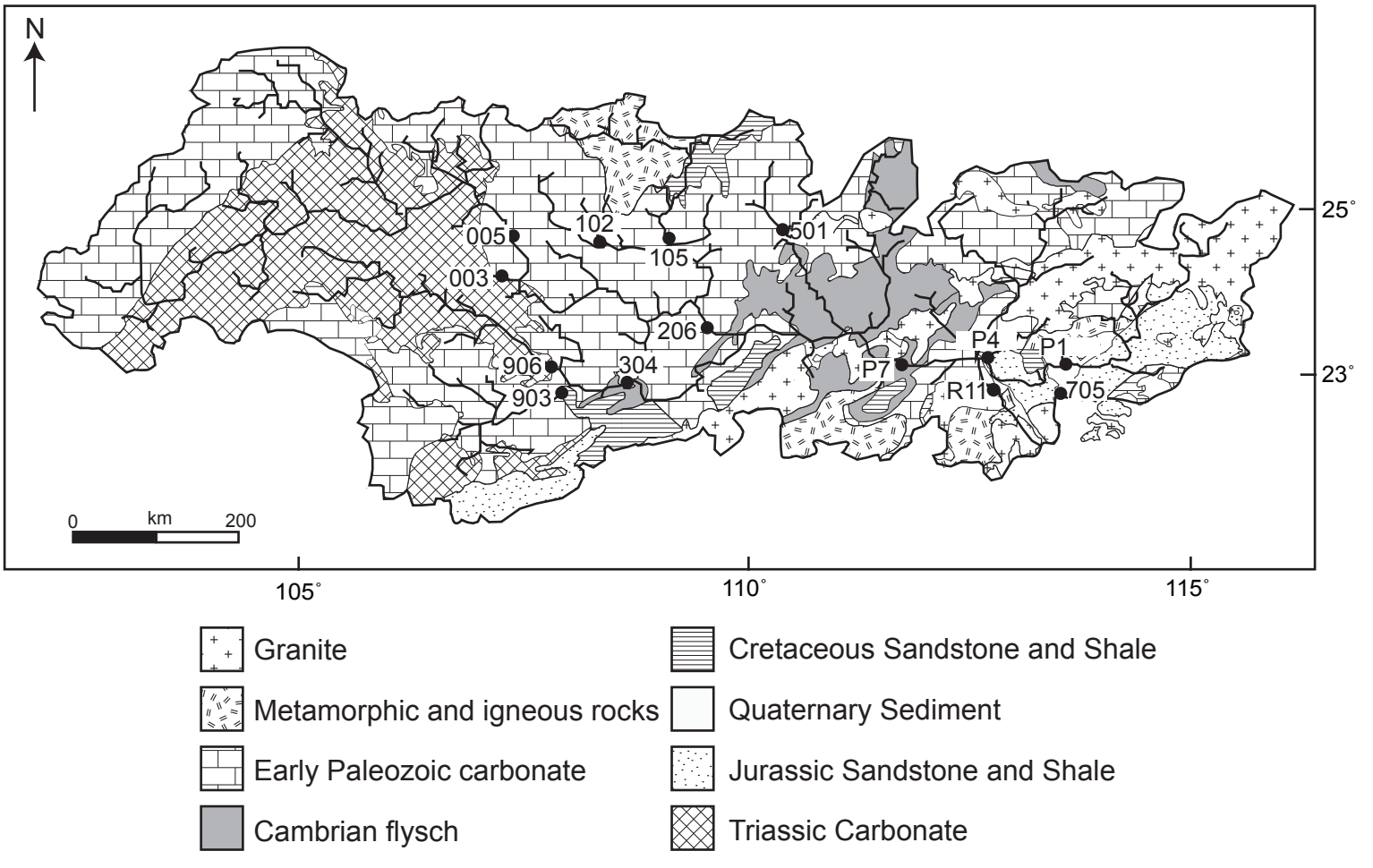

Figure 3
Liu et al

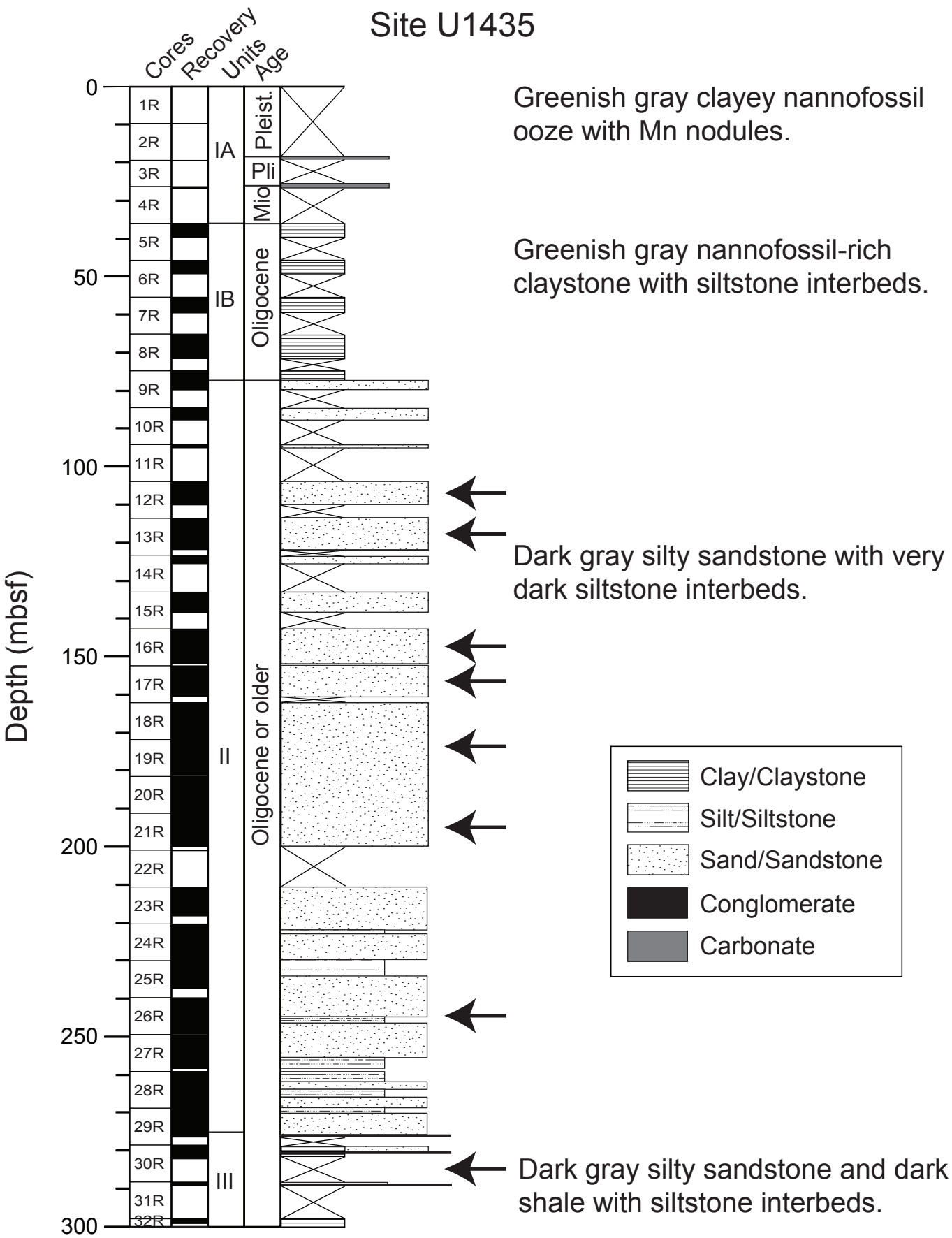

Figure 4
Liu et al.

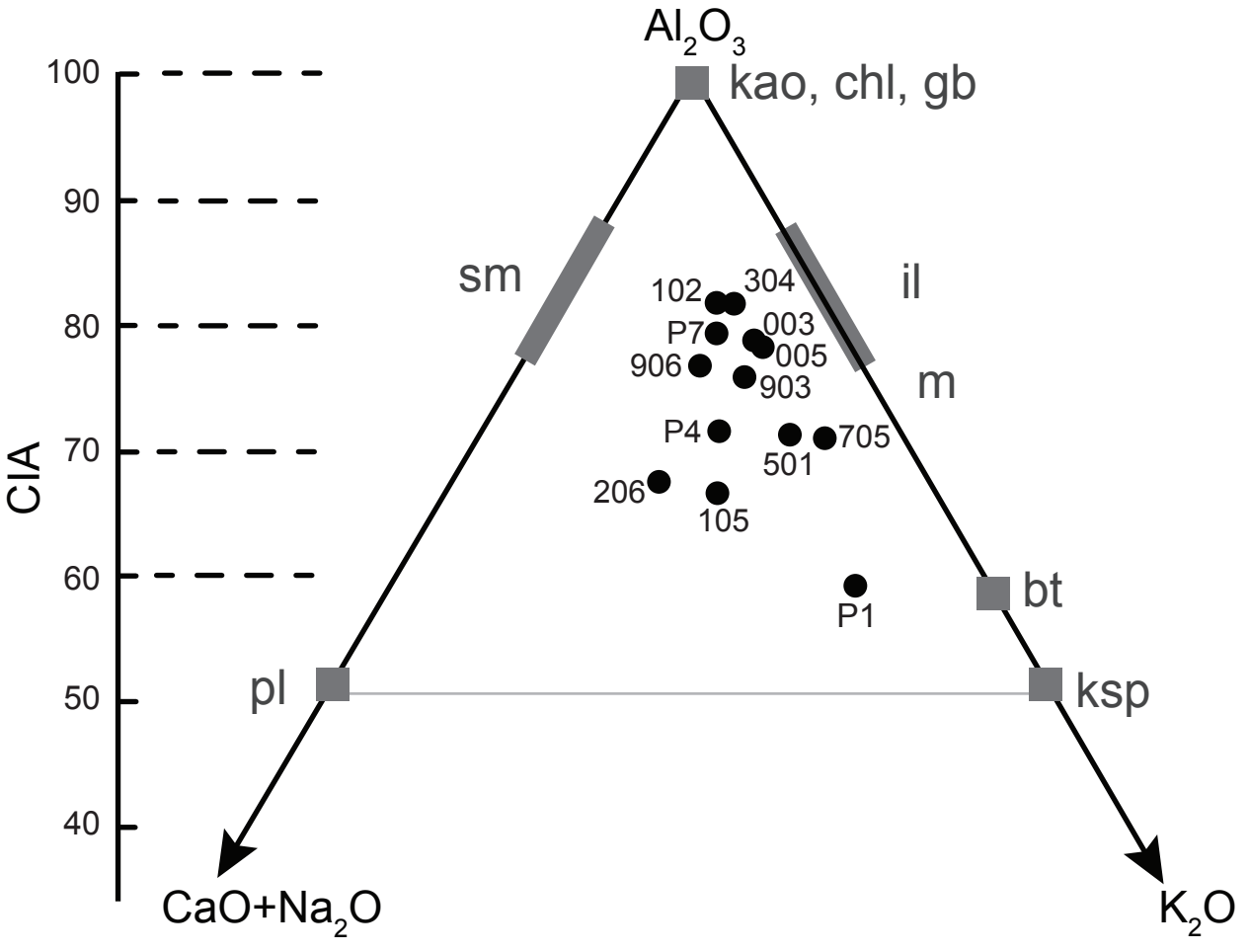

Figure 5
Liu et al

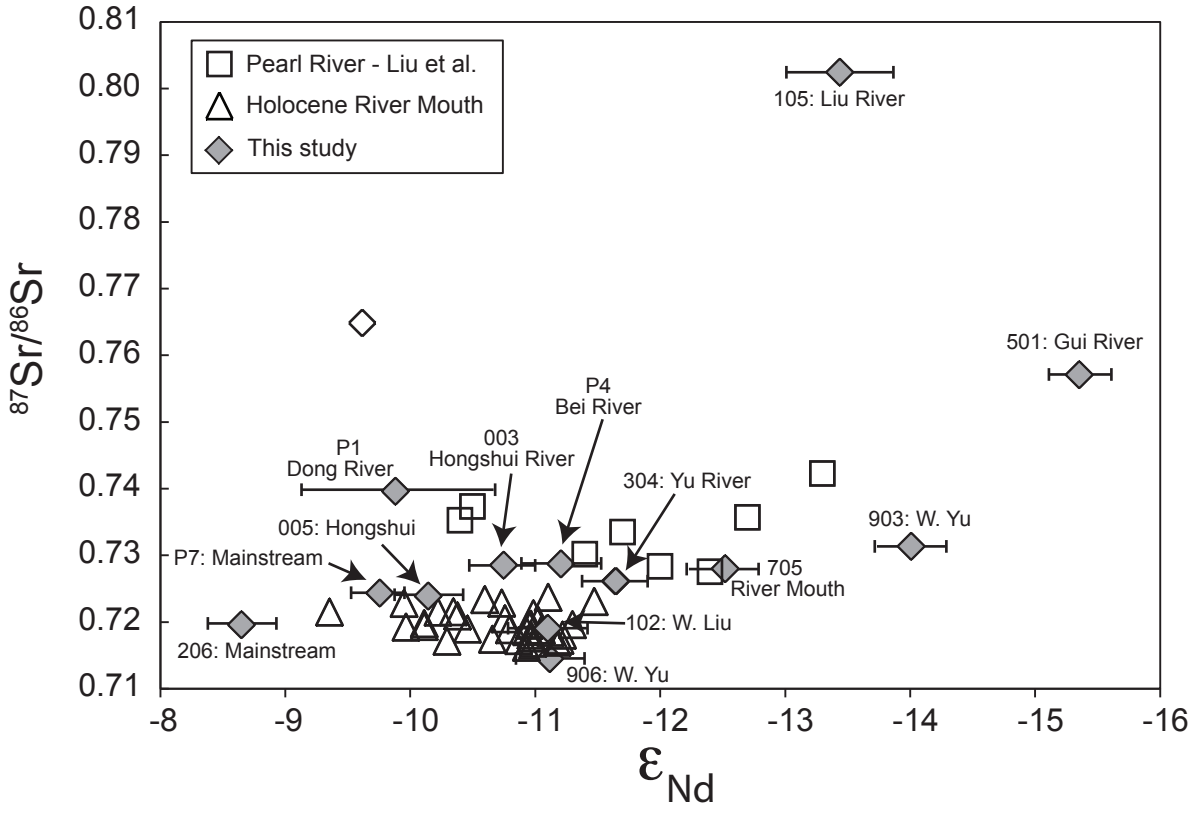

Figure 6
Liu et al

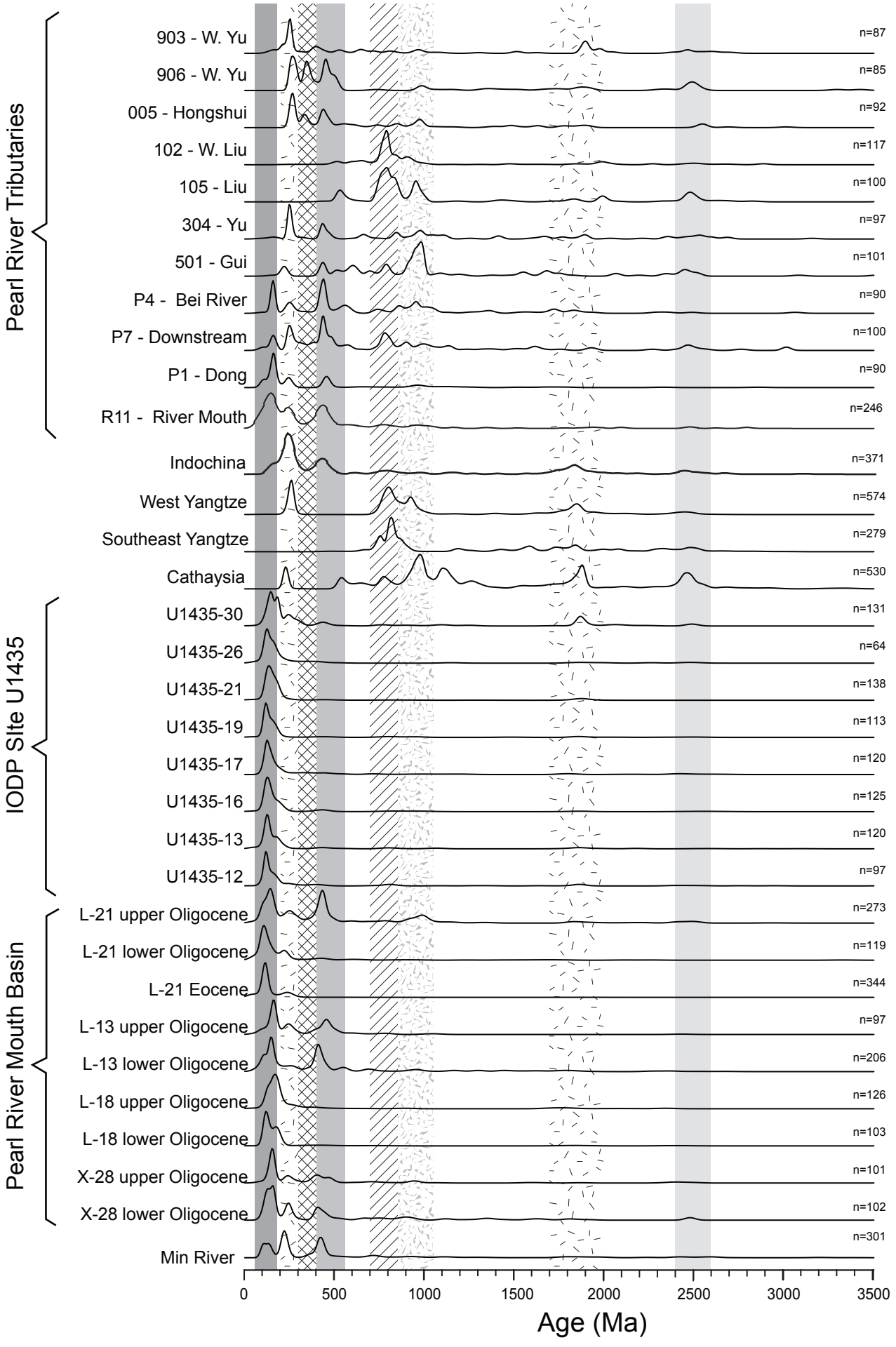

Figure 7
Liu et al

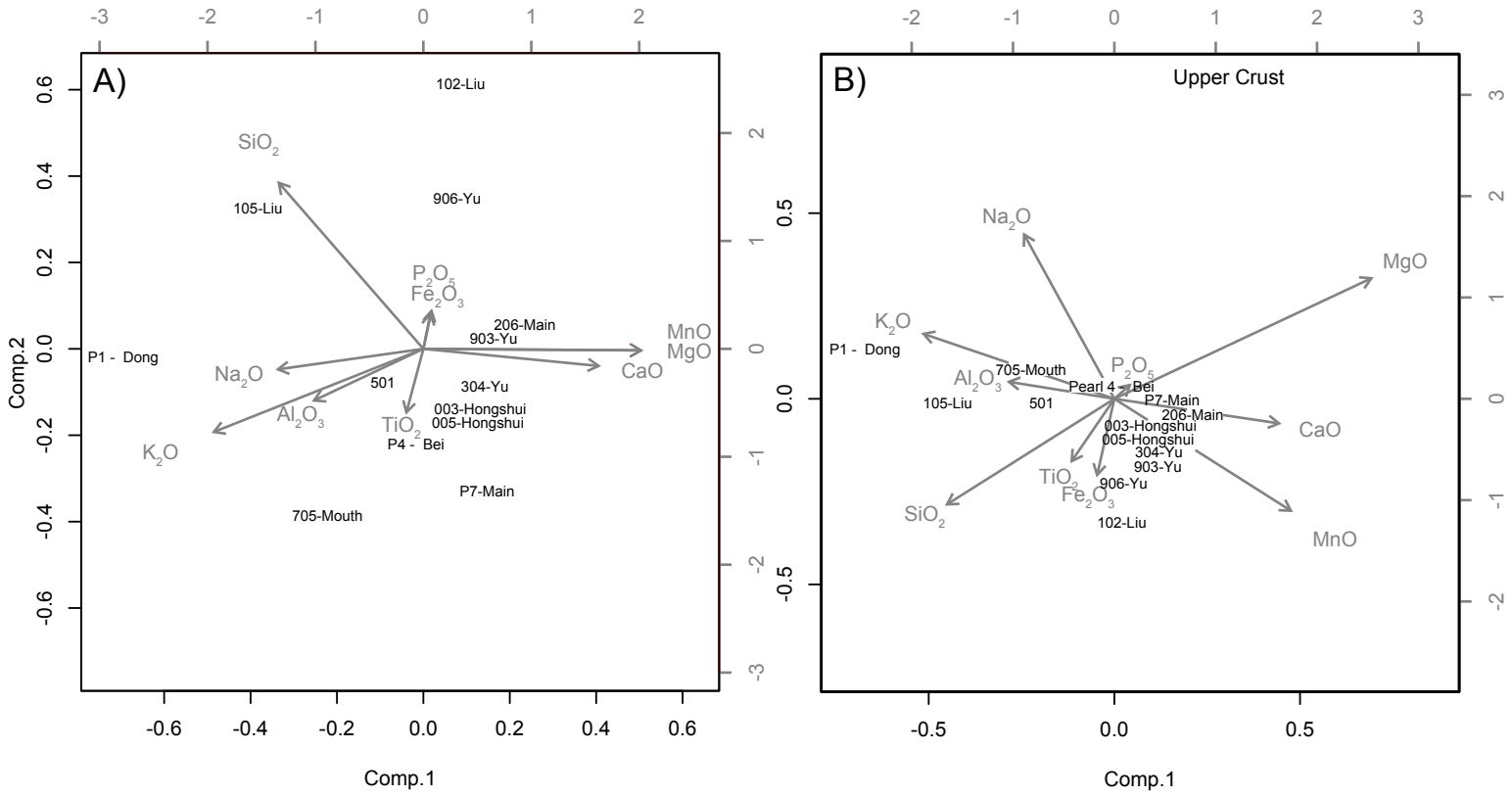

Figure 8
Liu et al.

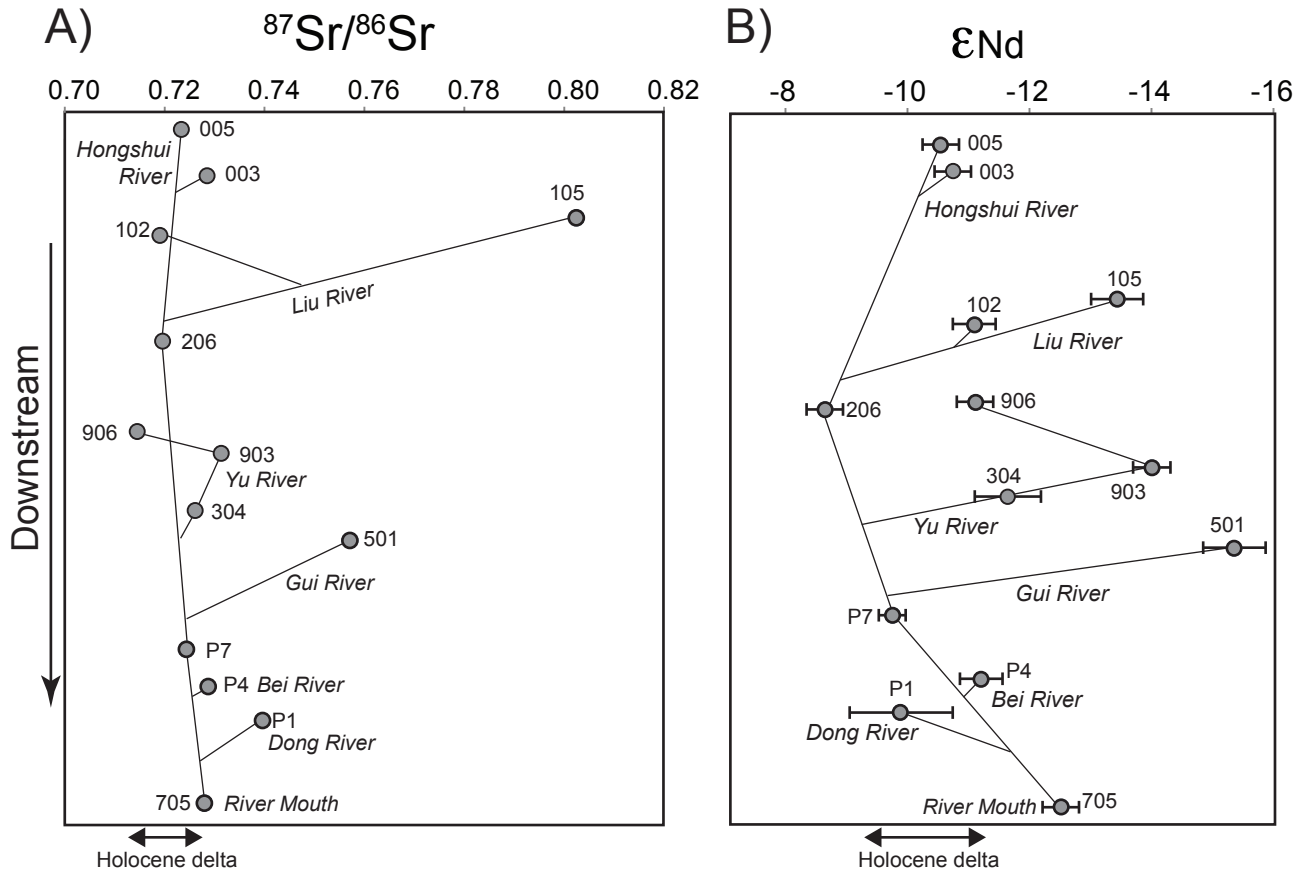

Figure 9
Liu et al

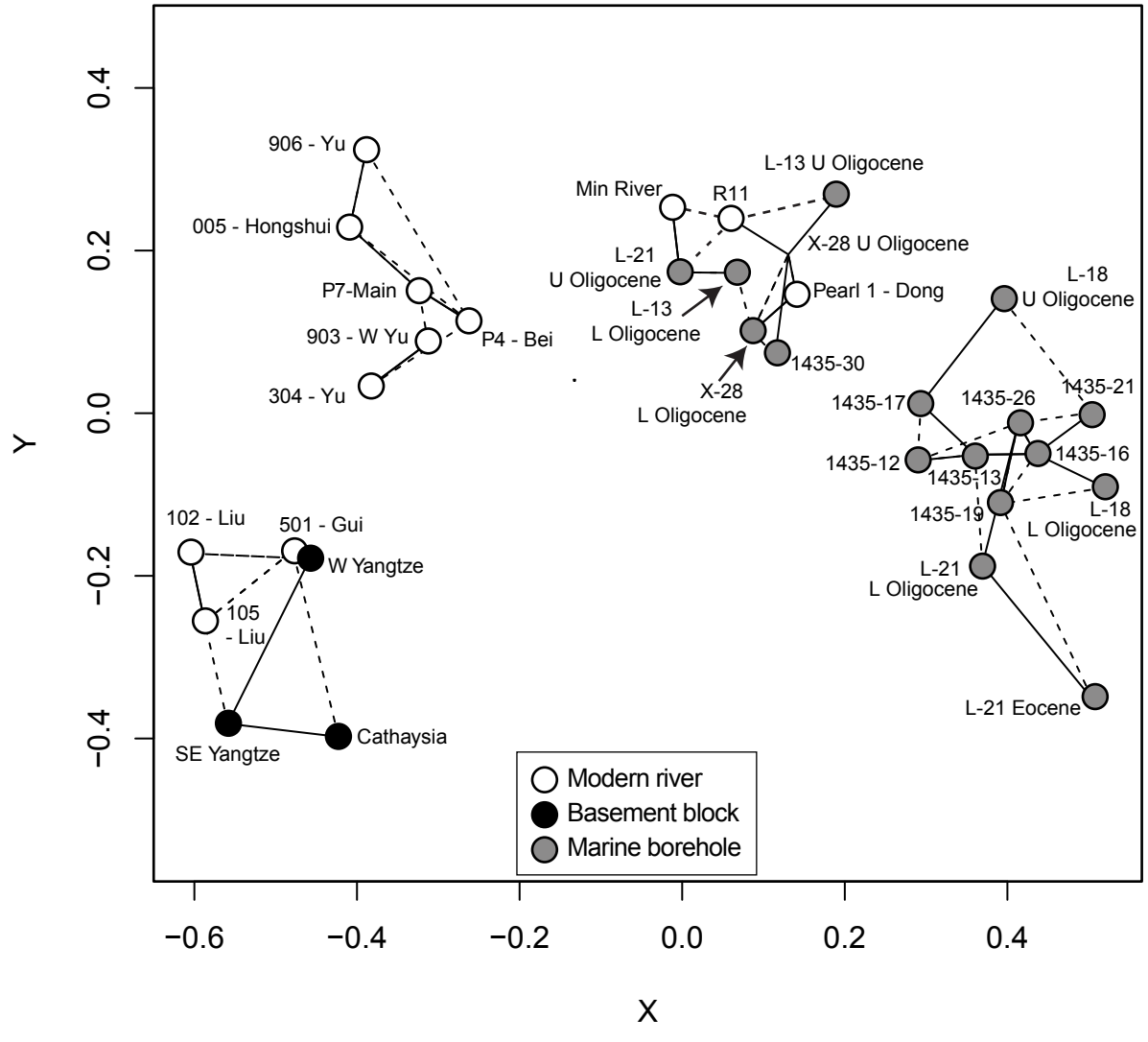

Figure 10
Liu et al

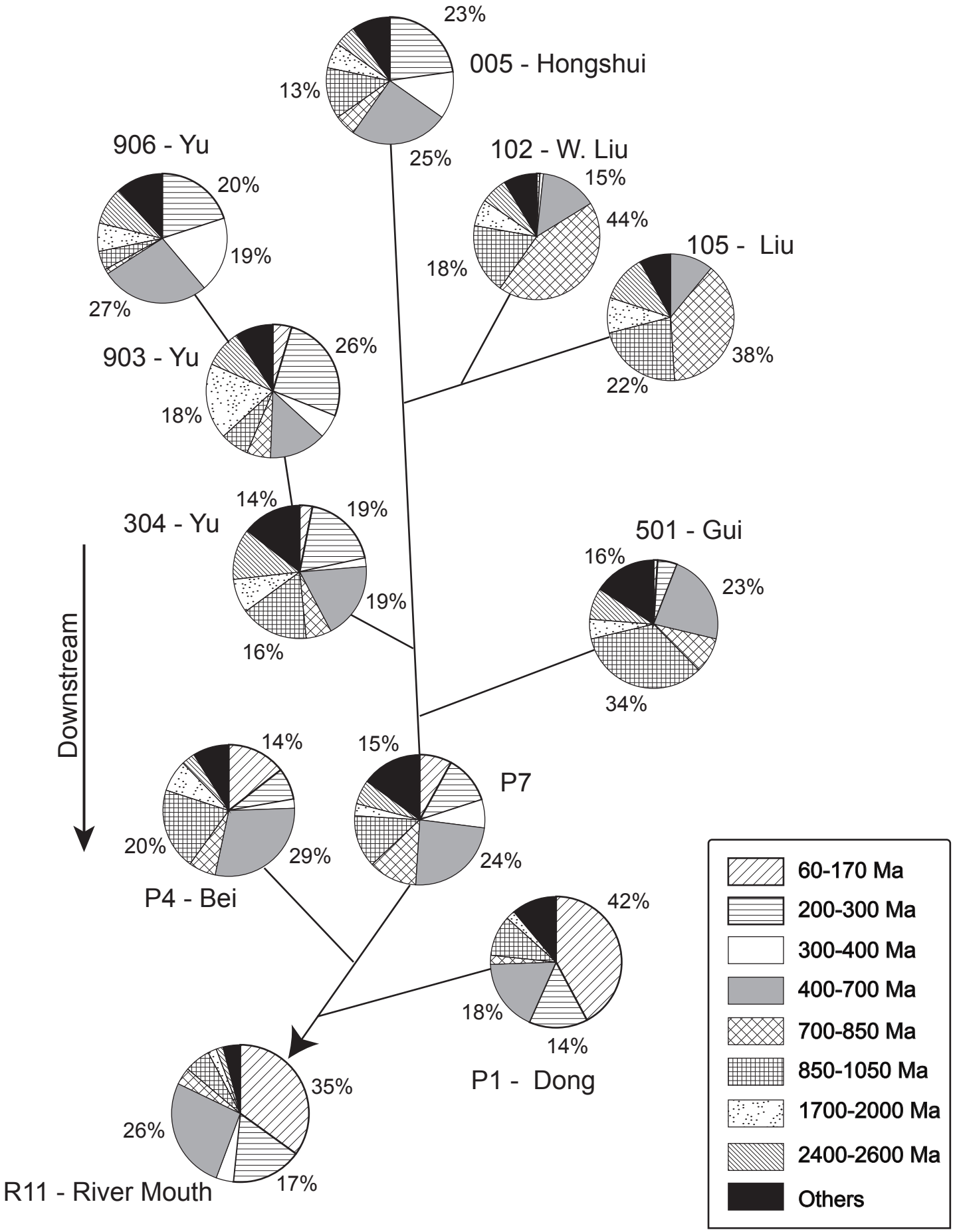

Figure 11
Liu et al.

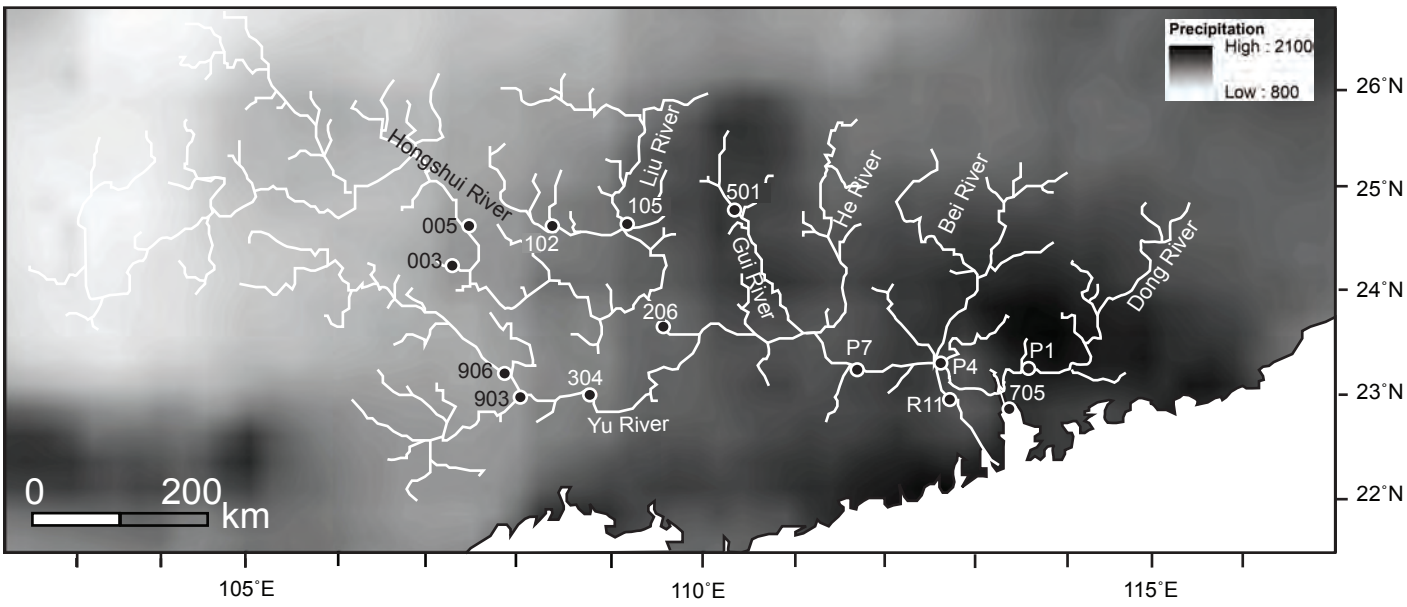

Figure 12
Liu et al

349 in order to constrain the source of sediment to the rift before the Oligocene. A combination of Nd and Sr isotopes show that the Gui, Liu and Dong Rivers are likely not important sources. Single grain zircon dates emphasize the importance of the westernmost tributaries, draining the highest topography and tectonically active areas as the primary sediment producers, namely the Hongshui and Yu Rivers. Our data indicate that climate is not the primary control on erosion patterns and intensities. Zircon dating also shows that the Gui and Liu Rivers are not generating large sediment yields. Discrepancies between this new data and earlier samples make the role of the Dong River hard to determine, although Nd isotopes suggest that it is not dominant. The source of sediment during the Eocene at IODP Site U1435 appears to have been a relatively local basement source, or a regionally restricted river only draining nearby areas of the Cathaysia Block, similar to but not identical to the modern Dong River. There is no evidence for a large regional river and we exclude sediment transport from the southwest, from Indochina. Our data are consistent with the idea of small drainage systems dominating the basin until the end of the Oligocene (~24 Ma), after which the Pearl River expanded towards its modern state as a result of headwater capture largely towards the West.

Keywords: zircon, isotope, erosion, provenance, Pearl River, South China Sea

Introduction

Drainage systems are born and develop in response to interactions between climate and tectonic processes. As new ocean basins open or mountain ranges rise drainages reorganize in response to the changing topography and discharge supplied as result of precipitation (Brookfield, 1998; Clark et al., 2004). In so doing they can be sensitive indicators of continental processes, which are then preserved in the sedimentary record within

50 basins supplied by those rivers. The major rivers of Southeast Asia have been the subject of
51 significant speculation in relation to their development, as a result of their proposed
52 interaction with the uplift of the Tibetan plateau (Clark et al., 2004; Clift et al., 2006; Zheng
53 et al., 2013). In this respect the Pearl River (Fig. 1) has typically been considered anomalous
54 in that it is generally not thought to have been involved in major headwater capture during
55 plateau uplift, but may be more closely tied to the development of the South China Sea (Clark
56 et al., 2004). In this study we assess the geographic diversity of sources within the modern
57 river in order to map crustal heterogeneity and to see where the modern river is deriving its
58 sediment. We then use this knowledge to interpret Eocene fluvio-deltaic sedimentary rocks
59 drilled within the South China Sea to determine how the Eocene Pearl River compares with
60 the modern. This then allows us to understand how the river has developed to the present
61 state.

62 The modern Pearl River Drainage (PRD) covers 8600 km^2 and flows across the
63 South China tectonic block, composed of both the Yangtze Craton and the Cathaysia Block
64 (Yao et al., 2013)(Fig. 2). The Pearl River is one of the major sediment sources to the
65 northern part of the South China Sea, although flux from Taiwan's many smaller rivers has
66 been significantly greater in the recent geologic past (Milliman and Meade, 1983). The
67 climate of the PRD is dominated by the East Asian Summer Monsoon, leading to maximum
68 discharge over the months of June-August (Zhang et al., 2012). The modern PRD is fed by
69 several tributaries (Fig. 1), with most of the catchment lying west of the river mouth and only
70 one major tributary, the Dong River, flowing from the east, as well as the Bei River flowing
71 from the north into the PRD.

72 In this study, we constrain the nature of the earliest paleo-Pearl River and attempt to
73 understand where the modern river is deriving the bulk of its load. In doing so we test what
74 factors control continental erosion. Debate continues as to the relative importance of

precipitation, seasonality, rock uplift, and lithology in controlling erosion (Bookhagen and Strecker, 2012; Bookhagen et al., 2001; Burbank et al., 2003). We use a combination of detrital zircon U-Pb dating and bulk sediment geochemistry to define the nature of sediment eroded in different parts of the modern PRD. These can then be compared to the modern river mouth to assess where the modern load is being derived. We also compare with zircon U-Pb dates from International Ocean Discovery Program (IODP) Site U1435 to see how the modern and ancient compare. If the Pearl River was comparable to the modern shortly after break-up then the zircon populations might be similar, assuming that Site U1435 was supplied by the paleo-Pearl River. However, if the Pearl River was either much smaller or larger than it is today during basin rifting, or if the site was supplied by a different river, then this should be apparent in the sandstones at IODP Site U1435. The pre-Oligocene sediments at IODP Site U1435 offer the chance to settle debate about the source of sediment into the active rift.

Geologic Setting

The PRD lies on the northern margin of the South China Sea, which started to extend in the Late Cretaceous, with renewed, stronger extension during the Eocene, and culminating in break-up and the onset of seafloor spreading after ~30 Ma in the vicinity of the Pearl River mouth (Briais et al., 1993; Cullen et al., 2010; Li et al., 2014). The underlying cause of the extension remains controversial and will not be discussed in this contribution. The bulk of the river's load has been preserved in the offshore Pearl River Mouth Basin (PRMB) and associated deep sag basins along the continental margin. The development of the PRMB can be classified into two parts, the syn-rift (56–30 Ma) and post-rift (<30 Ma) (Chen and Pei, 1993; Liu et al., 2016), although active extension in the PRMB continued until ~24 Ma (Clift

et al., 2002b). A total of nine formations have been defined on the basis of a series of transgressive and regressive cycles (Zhang et al., 2003; Zhu and Mi, 2010). During the syn-rift stage, three formations were deposited within the PRMB; the Shenhu (Ew_s), Wenchang (Ew_w) and Enping (Ew_e) Formations.

Three families of faults divide the PRD into several structural blocks, although at the largest scale the basement can be defined as comprising the Yangtze Craton to the north and northwest, and the Cathaysia Block to the southeast (Fig. 2). It is generally accepted that these two terranes collided ~800–1000 Ma (Wang et al., 2007) since which time they have formed a tectonically coherent South China Block. The geology of Cathaysia, especially in the far southeast, is dominated by Cretaceous granites and volcanic rocks linked to an active NW-dipping subduction zone of that age under the southern edge of Eurasia (Jahn et al., 1990; Sewell and Campbell, 1997). In contrast, the northwestern part of the PRD, which is mostly within the Yangtze Block, is mainly covered by Paleozoic carbonate (Fig. 3). Most of the catchment lies to the west of the river mouth and thus drains western Cathaysia. Two major tributaries, the Dong and Bei Rivers derive sediment from the eastern part of the Cathaysia Block. To the north the Gui River drains northern Cathaysia, while its neighbor, the Liu River, derives sediment from the Yangtze Craton, as well as Cathaysia. This block dominates the Beipan and Nanpan Rivers, which are the headwaters of the Hongshui River. The Yu River in the southwest part of the PRD drains the westernmost Cathaysia Block. Given the contrasting geological histories across these different tectonic terrains it is to be expected that sediment eroded from the different tributaries would have contrasting compositions and ages. In this study we employed the detrital zircon U-Pb dating method, together with bulk sediment geochemistry, to assess whether there are resolvable differences within the basin, as might be expected given the known ages of zircons in basement rocks from across the Cathaysia and Yangtze Blocks (He et al., 2013; Li, 1997; Wang et al., 2007; Xu et al., 2016).

We test whether the boundary between the tectonic blocks is really in the position previously determined and assess whether there is additional heterogeneity beyond that already understood.

IODP Site U1435, which is located in the northern South China Sea, is relatively close to ODP Site 1148 (Fig. 1), and may have received terrestrial material from both Taiwan and the Pearl River in the recent past. The oldest dated sample from IODP Site U1435 is considered to be Early Oligocene (~32 Ma; Unit 1B) overlying the sandstone at the base of the well (Unit II; Fig. 4) (Li et al., 2015b), which must be older and potentially useful in identifying any influence from a paleo-Pearl River.

Sediment Provenance

Sediment provenance in the PRMB since the Oligocene has been the subject of some debate, particularly concerning the influence of the Pearl River, compared to sediment transported along the coast from other sources, such as Taiwan, Luzon or even the Yangtze River. Local derivation from structural highs within the basin itself is an additional possibility. While Clift *et al*. (2002a) used Nd isotope data from Ocean Drilling Program (ODP) Site 1148 to argue for sediment delivery from southern China during the Oligocene, consistent with more recent work in Taiwan (Lan et al., 2014), Li *et al*. (2003) used the same type of data to propose that these sediments had flowed SW to NE from sources in Borneo at that time. Wei et al. (2012) used geochemical signatures from modern sediment to reinterpret the bulk geochemical results from ODP Site 1148 and advanced the idea that Oligocene (pre-26 Ma) sediment was being supplied from the North Palawan Continental Terrane, with no influence from a paleo-Pearl River. ODP Site 1148 is considered significant because it is located close to the continent-ocean boundary on the northern side of the basin (Fig. 1),

offshore from the PRMB, i.e., with the basin axis, and should be the recipient of sediment from a paleo-Pearl River, if it existed during basin rifting.

Shao *et al*. (2008) argued that a dramatic change in lithology seen in industrial wells drilled within the PRMB (Fig. 1) from a dominant silicate sediment source during the Oligocene to a carbonate source in the Miocene, was the result of the paleo-Pearl River drainage migrating westward through time, changing its sediment supply as it moved. A three part division of the PRD was proposed based on heavy mineral assemblages, as well as rare earth element (REE) compositions (Shao et al., 2015), suggesting that expansion of a paleo-Pearl River to the modern catchment should be resolvable from the sediments preserved in the PRMB.

Attempts have also been made to use clay mineral assemblages as indicators of provenance change within the PRD. A significant decrease in the relative importance of smectite between the Oligocene and the Mid Miocene has been detected by several earlier studies (Clift et al., 2002a; Tang et al., 2004). The dominance of smectite at ODP Site 1148 from 32 Ma to 23 Ma, following by a decrease and the low values after 15 Ma was interpreted to reflect chemical weathering of volcanic rocks on the flanks of the rift during the early post-rift period. An increase in the proportion of illite indicated erosion from metamorphic rocks located more within the continental interior, as the PRD expanded after break-up (Clift et al., 2002a). In contrast, Tang *et al*. (2004) interpreted the high smectite contents at ODP Site 1148 prior to 15 Ma to reflect weathering and erosion of igneous rocks erupted during seafloor spreading. In this case a reduction in smectite content starting at 23 Ma would then be interpreted to indicate a provenance change, which could be related to migration of the paleo-Pearl River drainage. Times of changing provenance can be correlated with some of the tectonic and climatic events that occurred during the opening the South China Sea (Shao et al., 2013), although it is not always clear how the tectonics would directly

impact the clay mineral assemblage. Care must however be used when using only clay minerals to undertake provenance studies because assemblages can change over millennial time scales driven by changing climate, often unrelated to provenance (Clift, 2016; Hillier, 1995; Thiry, 2000).

Some of the disagreement in results and interpretation of the various provenance proxies describe above may reflect the fact that different phases may be preferentially derived from certain source terrains or particular lithologies. The best provenance reconstructions are based on a number of proxies of which detrital zircon U-Pb dating is one of the most effective in this region (Clift, 2016). Nonetheless, we supplement this with combined Sr and Nd isotopes which have a proven record in sediment provenance in the South China Sea.

Sampling

13 medium to fine sand samples were collected from different tributaries of the modern Pearl River in order to determine what type of sediment each of these streams is contributing to the mainstream, and by comparison with the river mouth we can then isolate which tributaries are the most important in generating sediment (Fig. 1, Table 1). Although we only sample the coarser bedload and not the finer suspended sediment our sampling is expected to provide a representative image of the coarser sediment flux from each tributary. Because we also compare with sand offshore, and specially dense zircon grains that are transported as bedload our strategy is effective at tracing sand flux in the modern river. Whether this is the same as the finer grained suspended load is not addressed by this study. Sample locations and shortened identification numbers are summarized in Table 1. All 13 modern samples were analyzed for bulk major element and isotopic geochemistry, of which ten were also processed for U-Pb zircon dating.

196 Samples were also taken from IODP Site U1435. This site is located on a rotated fault
197 block, just north of the continent-ocean boundary and drilled a syn-rift sequence. Earlier
198 studies have established that extension intensified on the northern rifted margin in the
199 Eocene-Oligocene, suggesting that the sedimentary rocks considered here are of that age. The
200 maximum depth of the well reaches to ~300 m below the sea floor, with the section being
201 divided into three units (Li et al., 2015a). The top of the section is dominated by carbonate
202 and mudstone clearly deposited in deep water and in a distal setting. The sediments are dated
203 as Oligocene and younger based on microfossil evidence (Li et al., 2015b). The deeper part
204 of the section is devoid of datable marine microfossils, is harder to date and is consequently
205 assigned a pre-Oligocene age, likely Eocene. Water depths of sedimentation are interpreted to
206 be shallow continental shelf or deltaic, probably deposited close to a river mouth and in a
207 relatively high-energy environment based on the abundance of sand and current-related
208 sedimentary structures. Eight samples were selected for single grain U-Pb dating from Unit II
209 at Site U1435, with their locations shown in Figure 4.

210 The sandstones are relatively thick bedded and massive, and in turn overlie a short
211 and poorly recovered section of finer grained siltstone and shale (Unit III), which is
212 interpreted to be slightly more distal, possibly a deposit between active channels in a delta
213 system during the pre-Oligocene. Shallow water depths contrast with the deep water known
214 from the Oligocene at ODP Site 1148 (Shipboard Scientific Party, 2000), although the ages
215 may not the same. Because most models of extension predict deepening of water during
216 active rifting (Gawthorpe and Leeder, 2000) we presume that the sandstones at the base of
217 the site must reflect sedimentation during the early rift phase, predating the sediments at ODP
218 Site 1148 and are likely to be Eocene, based on regional understanding of the timing
219 extension in the South China Sea. Given their coastal or river mouth setting and location

offshore from the modern river mouth these sediments provide us the opportunity to assess if there was an early Pearl River and if so what its catchment may have been like.

Methods

Bulk Geochemistry

Although major element composition is rarely considered a good provenance proxy, since much of the crust has a similar andesitic bulk composition we determined the bulk sediment chemistry of the 13 samples from the Pearl River in order to determine their similarity, degree of chemical weathering intensity relative to fresh bedrock, and to assess the possible influence of hydrodynamic sorting on their bulk sediment chemistry when using other provenance methods. Because of limited sample size and the possible influence of diagenesis in affecting the IODP samples these were not analyzed for major element chemistry but were only subjected to detrital U-Pb zircon dating.

In contrast, bulk geochemistry analysis of the much larger modern Pearl River samples was performed at the University of Oldenburg, Germany. Major element composition was determined by X-ray Fluoresence (XRF), using a Panalytical Axios Plus XRF spectrometer routinely performed at ICBM. After a powdering a large representative volume of the original sediment 700 mg of material were removed and mixed with 4200 mg lithiumtetraborate, preheated overnight to 500˚C, fused to glass beads and analyzed with the X-ray spectrometer, which is calibrated against 65 standards from the Chinese IGGE series, French CRPG series, Japanese GSJ series, Canadian CCRMP series, German ZGI series and the USGS series.. Analytical precision and accuracy were checked with in-house standards

(PS-S, Loess, TW-TUC; e.g. Meinhardt et al. (2016)) and were better than 2% for major elements and 10% for trace elements. The results are shown in Table 2.

We choose to employ bulk sediment Sr and Nd isotopes to constrain the provenance of the sediment in the modern river. Nd is a robust provenance proxy, especially for finer grained sediment, because this element is generally immobile during weathering and erosion (Goldstein et al., 1984). Furthermore, recent work has shown that the Nd content of sediment is largely controlled by the Nd-bearing phases monazite and allanite that are not separated from each other by density-related mineral sorting during transport and so can be considered resistant to hydrodynamic processes (Garçon et al., 2013; Garçon et al., 2014). Nd has been used with apparent success previously in the northern South China Sea and Pearl River system (Clift et al., 2002a; Li et al., 2003; Liu et al., 2007). In contrast, Sr isotopes may be more susceptible to change during transport and are also affected by chemical weathering and the presence of carbonate (Derry and France-Lanord, 1996; Hu et al., 2013). These caveats make Sr isotopes a less reliable provenance tool, but when used in combination with Nd it can nonetheless be useful. Nd and Sr isotope data was not collected from the IODP samples because the grain size was sand-sized, which would require a large sample to derive a robust average that might have statistical meaning. Limited sample availability and small sizes meant that we chose to focus on zircon dating for determining the provenance of the older material as there was insufficient to measure bulk composition too.

Prior to total digestion all samples were leached overnight with 25% (v/v) acetic acid and 0.02 M hydroxylamine hydrochloride (HH) to remove carbonate-bound Sr as well as Nd and Sr contained in authigenic Mn-Fe-oxides. Hence, the Sr and Nd isotopic signatures is assumed to result solely from the silicate fraction. The leached samples and the certified standard BCR-2 (50 mg), as well as a blank, were treated with HNO_3 overnight to oxidize any organic matter. After that HF and $HClO_4$ were added and the vessels were heated for 12

h at 180°C. All acids were of suprapure quality. After digestion, acids were evaporated while the residues were redissolved and fumed off three times with 6N HCl, and finally taken up in 1N HNO_3.

From the resulting solutions, rare earth elements (REEs) and Sr were isolated from major elements and separated from each other by two-step column chemistry using Eichrom TRU-Spec resin. Nd was then isolated from interfering REEs using Eichrom LN-Spec resin with 0.23–0.25 N HCl as eluant. The TRU-Spec Sr-Rb cut was loaded on Eichrom Sr-Spec columns to isolate Sr using Milli-Q water. The isotopic compositions of Nd and Sr were analyzed on a Thermo Neptune Plus Multicollector ICP-MS at the ICBM, Oldenburg. For Nd isotope analyses, all samples were corrected for internal mass fractionation using $^{146}Nd/^{144}Nd = 0.7219$ and an exponential law. Each measurement session was accompanied by multiple analyses of the Nd standard JNdi-1 with sample-like concentrations, and $^{143}Nd/^{144}Nd$ ratios of all samples were normalized to the reported JNdi-1 value of $^{143}Nd/^{144}Nd = 0.512115$ (Tanaka et al., 2000). The Nd isotopic composition is expressed in ε_{Nd} notation, using the Chondritic Uniform Reservoir with a value of 0.512638 (Jacobsen and Wasserburg, 1980). The external reproducibility calculated for each session separately using the analyses of JNdi-1 was generally better than ±0.000015 or ± 0.3 ε_{Nd} units (2σ). The BCR-2 standard (n = 4) had an ε_{Nd} value of 0.1 (± 0.3, 2σ) well within the reported ε_{Nd} value of 0.0 ± 0.2 (Raczek et al., 2003). The procedural blank was ≤ 30 pg Nd.

For Sr isotope analyses, all samples were corrected for mass fractionation using $^{86}Sr/^{88}Sr = 0.1194$ and the exponential law. Measurements were accompanied by multiple analyses of NBS987 with sample-like concentrations, and $^{87}Sr/^{86}Sr$ ratios of all samples were normalized to the reported value of 0.710248 (Thirlwall, 1991). Monitored krypton "gas blanks", as well as Rb and Ba contents, were found to be negligible (Meinhardt et al., 2016). The external reproducibility is calculated using the analyses of NBS987 and was generally

292 better than 50 ppm (2σ). The BCR-2 standard (n = 4) had a $^{87}Sr/^{86}Sr$ ratio of 0.70502 ±
293 0.00004 (2σ) well within the reported $^{87}Sr/^{86}Sr$ ratio of 0.70496 ± 0.00002 (Raczek et al.,
294 2003). The procedural blanks were negligible throughout. Results are reported in Table 2.
295 Repeated digest of a random sample (in this case P7) yielded a difference in 0.3 ε_{Nd} units and
296 0.0004 % in the $^{87}Sr/^{86}Sr$ ratio (Table 2).

297

298 *U/Pb Detrital Zircon dating*

299 U-Pb dating of zircon is designed to determine the age of initial crystallization of
300 single zircon grains at high temperatures and has become a well recognized form of
301 provenance analysis as a result of the development of relatively inexpensive laser ablation
302 ICP-MS technology (Gehrels, 2014). Zircon is a U and Pb-rich heavy mineral, which is
303 relatively abundant in most crustal rock types, making it a useful mineral for dating
304 crystallization and cooling below ~750˚C (Hodges, 2003). Because of this high closure
305 temperature the U-Pb age is rarely reset by metamorphic events, allowing the mineral to be
306 used as a robust provenance indicator, while recognizing that reworking via older
307 sedimentary deposits can be an issue when matching detrital grain and bedrock ages (Carter
308 and Bristow, 2001).

309 Earlier analysis of bedrocks has shown that there are significant differences between
310 the spectrum of zircon U-Pb dates between the Cathaysia Block and the Yangtze Craton, and
311 even between the western and eastern parts of the Yangtze Craton (He et al., 2014; Li, 1997;
312 Li, 1999; Sun et al., 2009; Xu et al., 2016; Zhou et al., 2002). When these grains are
313 transferred by erosion to the river system then sediment derived from different source regions
314 can be resolved and by comparison downstream it is possible to identify which tributaries are
315 the most important in deriving sediment to the river mouth, if this signature in the age spectra

316 can be transmitted downstream. Of course zircon is unable to quantify erosion from zircon-
317 free carbonate bedrocks and this will result in an underestimation of erosion from the
318 carbonate-rich areas of the Yangtze Craton, but even in these areas there are still significant
319 volumes of siliciclastic bedrocks that can provide zircons to the river system.

320 Because zircon is relatively dense (4.65 g/cm^3) it also potentially has longer transport
321 times compared to quartz and feldspar (density 2.65 and 2.55–2.76 g/cm^3 respectively),
322 although both minerals may travel in the bedload (Resentini et al., 2013). Zircon travel times
323 in the Indus River (length 2900 km) have been estimated at 7–14 k.y. (Clift and Giosan,
324 2014). The Pearl River (length 2400 km) is somewhat flatter in gradient and might be
325 expected to have travel times longer than the Indus. Discharge in the Pearl River averages
326 9500 m^3/s, compared to 6600 m^3/s in the Indus, but because the Indus is sourced at >4 km
327 compared to ~2 km in the Pearl the transport capacity would be much greater. Although
328 insignificant on geologic time scales the travel times do need to be accounted for when
329 studying the modern river, as this may not be in equilibrium due to change in climate and/or
330 anthropogenic impacts. This means that zircon provenance work will reflect paleo-erosion
331 patterns that took place under different climatic conditions and with different patterns and
332 intensity of human settlement. This approach is less likely to be affected by 20th century
333 damming of the river, which has an immediate impact on the faster moving mineral species,
334 which is fortunate given the prevalence of damming through the PRD.

335 We attempted where possible to sample fine-medium grained sand so that similar
336 sediments in each tributary can be compared, and also be comparable to the zircons in
337 sandstones at IODP Site U1435. Although it might be expected that the oldest grains will be
338 preferentially found in the smaller size fractions because multiple phases of recycling will
339 tend to reduce crystal size through time as a result of abrasion, Malusà et al. (2016)
340 demonstrated that grain age distributions are independent of grain size, and not prone to

hydraulic sorting effects. In this study we target the 63–250 μm size fraction because this range has been proven to effectively yield the same distribution of all significant age populations present in the bulk zircon population in the Yangtze River (Yang et al., 2012) and we have no reason to believe that this is also not true in the PRD. It is also difficult to date grains much smaller than this range with current technology.

Detrital zircon grains were separated from sediment using heavy liquid and magnetic techniques. In the case of the modern Pearl River sample more than 1000 zircons are picked from each sample, weighing around 3 kg, of which 200 grains were selected randomly under a binocular microscope for dating, because around 100–120 grains are considered generally sufficient for characterizing sand eroded from a geologically complicated drainage basin (Vermeesch, 2004). The grains were mounted in epoxy and then polished. Cathode-luminescence (CL) images are taken using a Scanning Electron Microscope at the Chinese Academy of Science in Beijing and analysis was preferentially done on the grain cores. U-Pb measurement was accomplished using an Agilent 7500a Laser Ablation ICP-MS at the State Key Laboratory of Geological Processes and Mineral Resources, China University of Geosciences, Wuhan. Zircon standard GJ-1 (Jackson et al., 2004) was analyzed as a secondary age standard. NIST SRM 610 was used as an internal calibration for the laser ablation to correct the time-dependent trace element shift. 91500 zircon (Wiedenbeck et al., 1995) was run every 5–6 samples as an external calibration to correct the time-dependent shift of U-Th-Pb (Liu et al., 2008). Results from LA-ICP-MS with isotopic ratio were calculated using ICPMSCaldata 99 (Liu et al., 2010) and are shown in Table S1 (online data supplement). Based on Compston's convention, grain ages older than 1 Ga were determined by using $^{207}Pb/^{206}Pb$, while ages younger than 1 Ga were calculated from $^{206}Pb/^{238}U$ (Compston et al., 1992). Data with discordance greater than 15% were filtered out.

Samples from IODP Site U1435 (each 50cm^3) were analyzed by the U-Pb method at the London Geochronology Centre at University College London. To avoid bias in the separation process polished slides were made from the impure heavy fraction of diidomethane separation of the fraction < 300µm. Analyses were made on a New Wave Nd:YAG 193 nm laser ablation system, coupled to an Agilent 7700 quadrupole ICP-MS. The outer regions of zircons were targeted, rather than the cores in order to capture the most recent zircon growth events.

Real time U-Pb data were processed using GLITTER 4.4 data reduction software. Repeated measurements of external zircon standard Plesovice (TIMS reference age 337.13±0.37 Ma)(Sláma et al., 2008) and NIST 612 silicate glass (Jochum et al., 2011) were used to correct for instrumental mass bias and depth-dependent inter-element fractionation of Pb, Th and U. Temora (Black et al., 2003) and 91500 (Wiedenbeck et al., 1995) were used as secondary standards. As for the modern Pearl River sediment we used Compston's convention concerning preferred ages and the degree of discordance. Zircon U-Pb age and analysis results of IODP Site U1435 are shown in Table S2 (online data supplement).

Results

Bulk sediment chemistry reveals a relatively normal, quartz-rich continental sand composition for all samples. On the A-CN-K plot of Fedo *et al.* (1995) the samples plot towards the A-K axis, away from the CN corner and show moderate to high values of Chemical Index of Alteration (CIA) (Fig. 5). This indicates that the sediments are moderately to strongly altered compared to their bedrock sources. Chemical Index Alteration is calculated following Nesbitt and Young (1982), using the equation shown below,

$$CIA = \frac{Al_2O_3}{Al_2O_3 + CaO^* + Na_2O + K_2O}$$

CIA is a commonly used tool to measure the strength of the hydrolysis process, originally for soils, by comparing the remnant mole weight of water-immobile Al in the sediment and other

water-soluble elements. Higher CIA values, corresponding with more Al in the sediment, represent stronger leaching during erosion and sediment transport. While lower CIA values indicates less altered sediment with less mobile element leaching by hydrolysis. The samples from the different tributaries of the Pearl River have a wide range of CIA values ranging between 65 and 82, with the exception of sample P1 (Dong River), which has a low value of 59. Figure 5 highlights the strong alteration experienced by Samples 102 (W. Liu) and 304 (Yu River). These values overlap with and are slightly less than the range reported Liu *et al*. (2007) for fine grained sediment from the Pearl River.

$^{87}Sr/^{86}Sr$ and ε_{Nd} results are shown in Figure 6. $^{87}Sr/^{86}Sr$ values mostly vary between 0.72 and 0.74, similar to, but slightly lower than the range reported by Liu *et al*. (2007) for finer grained sediment in the same river. Conversely, our $^{87}Sr/^{86}Sr$ values from the modern Pearl River are generally slightly higher (0.71452 to 0.80241) than those found in Pearl River Holocene sediments (mostly 0.71620 to 0.72156 prior to 2.5 ka) (Hu et al., 2013). There are two exceptions to this trend, Sample 105 from the Liu River and Sample 501 from the Gui River, both of which drain from the north from the boundary between the Yangtze and Cathaysia Blocks. ε_{Nd} values also show a large range from -8 to -16. The most negative ε_{Nd} values are found in Sample 501 from the Gui River, while the most positive ε_{Nd} is from sample 206, which lies in the downstream region of the Yu River. In general the $^{87}Sr/^{86}Sr$ and ε_{Nd} values form a general array, with more negative ε_{Nd} values associated with higher $^{87}Sr/^{86}Sr$ values. Again Sample 105 from the Liu River is an exception in falling off this trend.

Results of U-Pb detrital zircon dating are presented in the form of Kernal Density Estimation (KDE) plots in Figure 7 (Silverman, 1986; Vermeesch, 2012). A number of different clusterings of ages are seen within the data. These population groups are defined visually as 60–170, 200–300, 300–400, 400–550, 700–850, 900–1050, 1800–2000, and

2400–2600 Ma. Although some grains fall outside these groups these are not numerous and are not considered diagnostic of provenance. The Yu and Hongshui Rivers are characterized by prominent 200–300 Ma (Indosinian) and 400–550 Ma (Caledonian) peaks. In contrast, the Liu River samples show few grains of these ages but common 700–850 Ma (Jinningian) grains. The neighboring Gui River is marked by a dominant population at 900–1050 Ma. In the SW of the PRD the Yu River has common 200–300 Ma and some 400–550 Ma grains. Further east both the Dong and Bei Rivers have a clear 60–170 Ma population, with lesser amounts of the 200–300 and 400–550 Ma groups. Not surprisingly the lowermost mainstream samples show several of these populations (e.g., P7), although the river mouth sample (R11) from Zhao *et al*.(2015) is dominated by grains in the 60–170 and 400–550 Ma ranges. In comparison, the zircons from all samples from IODP Site U1435 have a relatively simple spectrum dominated by 60–170 Ma grains, with the oldest sample (U1435-30) also containing a modest number of slightly older grains (200–300 Ma). The youngest zircon grain found was dated at 37 Ma, consistent with the Late Eocene-Oligocene depositional age inferred from the syn-rift stratigraphic location.

Discussion

Major Element Composition

The major element composition of the different samples can be compared using a Principal Component Analysis that investigates the range of concentrations in the different elements to see how similar the samples are to one another. This is an effective way to assess large-scale differences that might be caused by hydrodynamic sorting, rather than source composition,. Figure 8A shows the result of this analysis, made using the *Provenance* routine of Vermeesch *et al*. (2016). We also compare our sediments with the upper continental crust

439 average of Rudnick and Fountain (1995)(Fig. 8B). The figure shows that all the sediments
440 plot away from the upper crustal average, because they are relatively sandy and have lost the
441 clay and silt-rich fraction, resulting in a more quartz-rich bulk composition than average.

442 Despite the general similarity compared to upper crust Figure 8A highlights the
443 differences and thus the possible effects of hydrodynamic sorting on mineralogy and bulk
444 composition. If strong sorting had occurred then heavy mineral proportions would be
445 significantly affected, influencing the bulk sediment chemistry. The horizontal spread picks
446 out Sample P1 (Dong River) as being relatively Na_2O-rich, and poor in MnO, CaO and MgO,
447 indicative of low heavy mineral content, probably caused by hydraulic sorting. Because
448 heavy minerals are generally mafic a high concentration of these will increase the TiO_2,
449 Fe_2O_3 and MgO proportion compared to other sediments. Samples 705 (River Mouth), P4
450 (Bei River) and P7 (lower reaches) show modest TiO_2 enrichments. Although zircons and
451 monazites would not affect the major element chemistry their concentration would also be
452 accompanied by higher percentages of other minerals that are denser than quartz and feldspar,
453 such as pyroxenes and amphiboles that do impact major element chemistry. The Liu River
454 sample 105 is seen to be SiO_2-rich. Likewise, samples 906 (Yu River) and 102 (Liu River)
455 are also quartz-rich, but also show modest P_2O_5 and Fe_2O_3 enrichment. In general however
456 the clustering of major element together indicates that these sediments are equally affected by
457 hydrodynamic sorting during transport.

458 CIA values have a wide range and span to lower values than the data reported by Liu
459 *et al*. (2007) from finer sediment. The observation of less altered material in our sands is
460 consistent with the idea that finer grained material tends to be more weathered than the sand
461 and coarser silt fraction. CIA by itself is poor provenance proxy because of the impact of
462 hydrodynamic sorting on the mineralogy and because of the progressive removal of unstable
463 phases with transport.

Sr and Nd isotopes

With the exception of Sample 105 (Liu River) the correlation of Sr and Nd isotopes is suggestive of a dominant provenance control over these isotope systems within the Pearl River (Fig. 6). Because Sr isotopes are fractionated by weathering whereas Nd isotopes are not (Derry and France-Lanord, 1996) the correlation of most of the samples means that provenance is dominating the Sr as well as the Nd isotope composition. The anomalous ε_{Nd} value of Sample 105 requires that the Liu River is not a major sediment contributor to the bulk sediment flux. Going oceanwards ε_{Nd} values fall in the mainstream from 206 to P7 and finally to 705 (Fig. 9). This trend indicates the progressive addition of more continental, ancient crust into the river along its course between those points. The Yu and Gui Rivers are the only major tributaries that have more negative ε_{Nd} values than the river mouth, suggesting that one or both of them could be contributors.

Figure 9A shows the gradual drift to slightly higher $^{87}Sr/^{86}Sr$ towards the river mouth. The extreme $^{87}Sr/^{86}Sr$ value of Sample 105 (Liu River) is noted and demonstrates that this stream lacks much influence on the bulk flow, although if the Liu tributary sampled by 102 is more representative then this stream could still be a significant supplier. That possibility is however ruled out by the Nd isotope data because both Liu River samples have more negative ε_{Nd} values than either Hongshui River sample, yet the mainstream, downstream of their confluence becomes more positive in ε_{Nd}, meaning that other more positive (unknown) sources dominate over the Liu River as sediment producers in the upper reaches. Sample 206 on the mainstream is the most positive sample, with no analyzed tributary capable for forcing the mixed composition to such a high ε_{Nd} value. We infer erosion from relatively primitive sources into the river either from undocumented tributaries or from the bedrock along the

mainstream itself. Some of the variability could represent short-term variability in the river load, possibly even seasonally driven.

The relatively negative ε_{Nd} values seen in the Yu, Gui and Bei Rivers are all consistent with the gradual drift of bulk composition to more negative ε_{Nd} values towards the delta downstream of each confluence. In contrast, the more positive ε_{Nd} value of the Dong River compared to the river mouth (705), would suggest that this is not affecting the bulk composition greatly downstream of P7. Why the mainstream becomes as negative as it does is not clear from this study because the river mouth is even more negative than the Bei River, which is the most oceanward major tributary sampled. Either our samples are not truly representative of the flux or there are other sources, local or small tributaries, that are adding sediment with relatively negative ε_{Nd} values in the lower reaches and which we have yet to measure. This latter option seems unlikely because of the generally positive ε_{Nd} values known from bedrocks close to the Pearl River mouth (see synthesis by Hu *et al*. (2013)). The Gui River ε_{Nd} value is so negative compared to the mainstream both upstream and downstream of that confluence that this cannot be a strong supplier of materials. Nd isotopes can be sensitive to hydraulic sorting effects because a handful of monazite grains concentrated by their high density in a sample can completely change the isotopic composition over short distance.

The modern river mouth (705) is somewhat more negative in ε_{Nd} value compared to the Holocene delta samples (Hu et al., 2013) or to the modern river samples of Liu *et al*. (2007), indicative either of a change in sediment yield patterns in the recent past, perhaps driven by farming or damming practices, or that Sample 705 is not the most representative of the average flux from the river to the South China Sea, which seems most likely.

We further consider how the Nd isotope data from onshore can help understand the Nd evolution previously analyzed at ODP Site (Clift et al., 2002a; Li et al., 2003). This shows

512 a long-term fall in ε_{Nd} values from greater than -8 to around -10.5 from 29 Ma to the present.
513 The fall is especially marked between 22 and 10 Ma. ε_{Nd} values of -8 would correlate closest
514 with the Dong River and essentially exclude my sediment supply from most of the
515 isotopically negative tributaries at ~29 Ma. Sediment could have bee supplied from a paleo-
516 Dong River or from other smaller rivers that also drained Mesozoic plutons and volcanic
517 rocks similar to those on the Dong basin. The subsequent evolution to ε_{Nd} values of around -
518 10 could be achieved by expansion of the drainage to one closer to the present, involving
519 tributaries with more negative ε_{Nd} values.

520

521 *Zircon U/Pb of the Pearl River*

522 The general predictions of sediment production derived from bulk sediment analysis
523 can be further explored using the U-Pb zircon age spectra from the different samples and with
524 reference to the known spectra of basement rocks within the Cathaysia and Yangtze Blocks.
525 When two rivers with different spectra come together the composition downstream should
526 reflect which river is dominating the sediment flux of the joint stream. However, zircon
527 concentrations in different tributaries, reflecting the relative fertility of source bedrocks,
528 affects the way that this method can be used to determine relative sediment yield across the
529 basin The carbonate dominated west of the catchment contrasts with the volcanic rocks and
530 granites in the east (Fig. 3). This factor can be accounted for if an effective way can be found
531 to estimate relative abundance. This may include point counting of heavy mineral suites, or
532 the use of Zr concentrations as a proxy for the amount of zircon in a given sediment (Amidon
533 et al., 2005).

534 In our study Zr concentrations range from lows of 45 ppm in samples from the Yu
535 (906) and Liu (105) Rivers, up to 668 ppm in the modern river mouth (705), and 552 ppm in

536 the Yu River (903) just downstream from low concentration sample (Table 2). At face value
537 this would require major corrections when performing mixing calculations. However, this
538 also presumes that the sediment samples taken are representative of the river at the point of
539 sampling. As we were sampling at the river bank for the most part this seems unlikely,
540 because dense zircons might be expected to be concentrated in the thalweg in the stream
541 center, and could vary greatly in concentration across a single sand bar, or around a meander
542 bend because of current sorting. Although the principal component analysis (Fig. 10) argued
543 against large compositional differences between most samples (except for the Dong River)
544 there is still significant uncertainty in the hydrodynamic effects in terms of zircon
545 concentrations because zircons do not impact the major element chemistry. Consequently, in
546 this study we opt not to make a correction for zircon concentration, because any weighting
547 based on the bulk chemical analysis is just as likely to introduce new errors than remove
548 existing problems. In the following discussion we assume that the zircons are representative
549 of the total sediment flux assuming relatively uniform concentrations in the bedrock sources.
550 Our budget will be biased if this assumption is not true over large areas of the drainage basin.

551 The KDE plots in Figure 7 show that there are very few 700–850 Ma grains in the
552 river mouth sample (R11) from Zhao *et al.*(2015), and only a moderate number in the lower
553 reaches Sample P7. Because these grains are uniquely common to the Liu River these data
554 argue against that stream being a large contributor to the bulk sediment flux, consistent with
555 the Nd data. The river mouth (R11) does however show a clear 60–170 Ma population that is
556 largely supplied by both the Bei and/or Dong Rivers, although with possible additional
557 erosion of bedrock sources in the lower reaches as well. Although the river mouth also
558 includes many 400–550 Ma grains these are common in many Pearl tributaries and do not
559 allow a constraint to be placed on the sedimentary budget. Interestingly, the river mouth
560 sample does not bear much similarity to any of the compilations from the bedrock sources of

561 the Yangtze Block and Cathaysia (He et al., 2013), probably reflecting heterogeneity within
562 these blocks that makes comparison at the very largest scale pointless. The 200–300 Ma
563 group that is known from Cathaysia and the W Yangtze Blocks, but not the SE Yangtze
564 Block (Fig. 7), is clearly important to the Pearl River, but the relative dearth of 700–850 Ma
565 grains in the Pearl, despite their abundance across the Yangtze Block, suggests that this
566 terrain is less important as a sediment supplier than Cathaysia. The Yu and Hongshui Rivers
567 are the greatest source of 200–300 Ma grains and their frequency in the lower reaches and
568 river mouth favors these streams as significant sediment producers.

569 The multidimensional scaling (MDS) analysis of Vermeesch (2013)can be used to
570 compare the entire U-Pb age spectra of different samples from within the Pearl River system
571 in order to constrain the provenance of the zircon grains. Figure 10 shows that the lower
572 reaches mainstream (P7) is most like the Hongshui, although it is quite close to the Yu River
573 samples as well, so that both tributaries are implicated as dominant sources. This also implies
574 that the Gui and Liu Rivers are not sediment productive, at least with regard to zircon. The
575 Gui and the Liu do however show similarity with the bedrock compilations from both parts of
576 the Yangtze Block and Cathaysia. This means that there are many basement sources that have
577 not been properly characterized within the PRD. In turn this means that provenance
578 interpretations based only on comparison between bedrock source and sediment data are
579 likely to be in error.

580 It is noteworthy that zircon age data from the river mouth sample (R11) plots closest
581 to the Dong River, implying strong flux from that tributary. However, this is not realistic
582 because the Dong River joins the Pearl River mouth on the opposite side of the distributary
583 network of the delta compared to R11 and could not be supplying this location (Fig. 1B). In
584 any case strong flux from the Dong River is at odds with the bulk sediment Nd isotope data
585 (Fig. 6). If there was large sediment supply from the Dong that would influence the zircon

586 population then it would reasonably be expected to change the bulk sediment Nd and Sr
587 isotope character too, unless the source of the Nd-rich monazite was quite different from the
588 source of zircons which is unlikely in drainage basins as large as those considered there. The
589 river mouth samples plot far from the Dong River in Figure 6. It is possible that R11 is
590 heavily influenced by local sediment sources from the eastern Cathaysia basement that also
591 supplies the Dong and Min Rivers and is not representative of the true average flux to the
592 ocean. Mixing of P7 and the Bei River might produce a mixed sediment more like R11, but
593 the MDS plot suggests this is unlikely and the two rivers do actually flow together at the
594 present time.

595 If P7 is actually a better estimate of the net discharge to the ocean than R11, then the
596 zircon ages would be consistent with the Nd isotopes at Sample 705 in arguing that most of
597 the sediment to the South China Sea is eroded in the Hongshui and to a lesser extent the
598 Western Yu River basins. If both the Nd and U-Pb data sets are valid and correct, as we
599 assume, but also contradictory then this would require the Nd-bearing phases (mostly
600 monazite and allanite (Garçon et al., 2014)) to be moving through the river at a different
601 speed than the zircon so that the river would be in a state of disequilibrium in terms of
602 erosion/sediment transport patterns. What is clear is that the Hongshui ± Yu are the most
603 sediment productive part of the western PRD.

604 Zircon age evolution downstream can also be seen by simplifying the age spectra into
605 a pie diagram and seeing how these change downstream. In Figure 11 the age structure is
606 simplified into the groupings discussed above and connected in a network to show change
607 with transport. We particular note that the lower reach sample P7 is very similar in its basic
608 divisions compared to Samples 005 (Hongshui) and to 304 (Yu), as implied by the MDS plot.
609 Although the lower reach sample P7 contains 60–170 Ma grains not found in these upper
610 stream samples this just reflects further modest sediment influx to the mainstream in the

middle and lower reaches. The Liu and Gui Rivers are again clearly anomalous in being unlike any other samples in the mainstream. Their confluence does not significantly affect the composition of the mainstream. The Yu River changes significantly between Samples 906 and 903, but not so much from that point to 304. This means that sediment production is most important in the upper reaches of the Yu River and diminishes downstream.

The overall interpretation from all data sets considered together is that the headwater regions, especially in the Hongshui and Western Yu River are producing much of the sediment in the Pearl River, west of the river mouth. Because of the complicated distributary patterns in the river mouth area, which are unstable (Fig. 1B), the influence of the Dong River is unclear. Zircon data suggest that the Dong is important but the Nd argues against that. Considering just the western parts of the PRD it is apparent that topography coupled with greater seismic activity is controlling the erosion patterns within the basin. NASA's Tropical Rainfall Measuring Mission (TRMM) records the highest annual precipitation in the area around the Pearl River mouth (>2.1 m/yr) and the lowest to the west (1.0–1.5 m/yr)(Fig. 12). If rainfall alone was the primary driver of erosion then erosion should be highest in the east, while at least within the western PRD the erosion is associated with the highest and steepest topography, as well as zones currently experiencing active faulting, as measured by earthquakes >4.5 magnitude (Ekström et al., 2012), and tectonic uplift linked to uplift of the outer edge of the Tibetan Plateau, as measured by GPS (Chen et al., 2000).

Implications for Crustal Structure

Although the large-scale division of southern Chinese bedrock geology into Yangtze Craton and Cathaysia is well established (Kusky et al., 2007) our work reveals greater diversity that can be important when assessing the source of sediments to the South China

635 Sea. As described above, some tributaries are especially rich in zircon grains with a given age
636 range. This is useful not only to pinpoint the possible source of sediment in the final
637 depocenter or delta but also in showing divisions within the crust of southern China. We do
638 not dispute the generally accepted location of the Yangtze-Cathaysia suture, for example
639 from Pubellier *et al*. (2008) or Kusky *et al.* (2007) but we also see important subdivisions
640 within that greater subdivision.

641 The Liu River is dominated by ~800 Ma grains associated with the collision between
642 Yangtze Craton and Cathaysia (Wang et al., 2007). Samples 005 and 906, from the Hongshui
643 and Yu Rievrs respectively are both very rich in Caledonian (400–550 Ma) grains (40–50%
644 of the resolvable grain population). They also contain significant quantities of 200–300 Ma
645 grains, linked to the Indosinian Orogeny, and likely reworked from Triassic sandstones
646 deposited across the region after that series of tectonic and thermal events (Carter et al., 2001;
647 Lepvrier et al., 2004).

648 The Yu River increases its proportion of 200–300 Ma grains between Samples 906
649 and 903, indicating that the Indosinian-rich belt must run through this region, with
650 Caledonian (400–550 Ma) rocks located further west in the PRD. This allows sub-divisions
651 of complexity to be recognized within both the Yangtze and Cathaysia Blocks (Fig. 2).
652 Sample 903 (Yu) also reveals a source of relatively old (1700–2000 Ma) grains in the far SW
653 of the Yu River tributary that are rare, if not absent elsewhere in the basin (Fig. 2). Grains
654 <170 Ma are limited to source rocks around and east of P7, i.e., the eastern Cathaysia Block
655 (Fig. 2). Such grains are seen in P7 so there must be some source rocks of that age eroding
656 upstream of that point, yet the strongest influence can be seen in the Dong (P1) and Bei (P4)
657 Rivers. The fact that the Bei and Dong do not plot with the compilation of basement
658 Cathaysia on the MDS diagram (Fig. 10) testifies to the dangers of using only such
659 compilations for provenance analysis. The Dong and Bei River zircon ages are consistent

660 with the abundance of grains of 60–170 Ma age found in the Min River, which drains eastern
661 Cathaysia toward to the SE into the Taiwan Straits (Xu et al., 2016). Understanding what
662 type of bedrocks are available in different parts of the basin is important for provenance
663 interpretation of older sedimentary rocks. For example, the appearance of 700–850 Ma grains
664 does not necessarily mean a direct former connection between central and western China and
665 the Pearl River (Yu et al., 2015), but could reflect either headwater capture and/or intensified
666 erosion within the upper reaches of the Liu River.

667

668 *Zircon U/Pb Offshore*

669 We now consider the origin of the zircons from Paleogene sedimentary rocks from
670 IODP Site U1435, as well as data from similar aged sedimentary rocks from nearby industrial
671 wells within the PRMB (Shao et al., 2016), representing the more proximal areas of the
672 newly developing continental margin. As noted above the U-Pb age results from IODP Site
673 U1435 have similar distribution patterns in the KDE (Fig. 7), with most grains concentrated
674 at 60–170 Ma. The patterns are quite different from most of modern Pearl River tributaries,
675 except for Sample P1 (Dong River), implying a simple source restricted to rocks similar to
676 those found in the eastern Cathaysia Block, the source of the modern Dong River. The Dong
677 River sample does include some older grains not seen at Site U1435 indicating that the
678 drainage was more restricted and did not include the present Dong River drainage. Although
679 similar young U-Pb ages are also found in Palawan on the southern margin of the basin
680 (Suggate et al., 2014) this seems less likely to be a source because the rift had already
681 developed at this time and such sediment would have to cross the basin axis to reach IODP
682 Site U1435. Such transport would have become more difficult as rifting intensified.

683 The MDS plot shows that the IODP samples plot away from either the R11 river
684 mouth or the lower reaches sample P7 (Fig. 10). This requires that the Eocene at Site U1435
685 must have a different provenance than the modern Pearl River. The Site U1435 sediment lack
686 some of the older zircons seen in the Dong River, showing that this site was receiving
687 material from an even more restricted range of sources than seen by the modern Dong River.
688 Because the Cathaysia continental basement extends offshore under the rifted margin it is
689 quite possible that the rivers feeding IODP Site U1435 were relatively locally sourced within
690 the offshore basin, or from proximal sources nearby.

691 The oldest sample (U1435-30), shows slightly more diversity with some 200–300 Ma
692 and a small 1700–2000 Ma group (Fig. 7). The former group is found within the modern
693 Dong River but the older grains are less common, although they have been found within
694 Cathaysia basement rocks, as well as in Sample 903 from the SW Yu River, which drains the
695 hills along the coastal southern edge of the PRD. On the MDS plot Sample U1435-30 shows
696 close similarity to P1 (Fig. 10), implying that it could represent drainage from the immediate
697 area of southern China north of the modern river mouth or from a drainage with similar rocks
698 as the modern Dong River. The source of the sediment in U1435-30 is not hugely different
699 for the younger samples. The U-Pb zircon ages in Sample U1435-30 must still have been
700 largely local to the basin, but may indicate the provenance became more restricted during
701 sedimentation at the site, as the rifting progressed. Active extension might be responsible for
702 not only forming the sub-basin in which these sediments were preserved but also for uplifting
703 nearby fault blocks whose erosion could then dominate the sedimentation. There is no
704 suggestion of a large regional river at the time of sedimentation of the syn-rift units at IODP
705 Site U1435, either draining from southern China or from Indochina.

706 Wells L-21, L-13, L-18 and X-28 within the PRMB, immediately north of IODP Site
707 U1435 are selected from Shao *et al*. (2016) in order to understand how the sedimentation at

the IODP site fits into a regional context. Depositional ages of the sediment from these four wells span from Eocene to Oligocene. The KDEs show that many of the sediments share strong similarities in their U-Pb age spectra with those at Site U1435, especially having a prominent grouping at 60–170 Ma. The only Eocene sample from Well L-21 (i.e., age equivalent to the U1435 material) is essentially indistinguishable, consistent with a uniform source across the basin at that time. The MDS plot (Fig. 10) also indicates that both Upper and Lower Oligocene at Well L-18 have the same basic provenance as the U1435 sediment, suggestive of a consistent source from the north from eastern Cathaysia. Towards the west and further north Oligocene sediment from Well X-28 shows close affinity both with the Dong River and with Sample U1435-30 (Fig. 6). Located between IODP Site U1435 and Well X-28, Oligocene sediments from Wells L13 and L21 show a mixture of material from the local source than dominates Site U1435 and the slightly more diverse eastern Cathaysian sediments now found in the Dong and Min Rivers. There is no need for the mixed sediments were actually supplied from a paleo-Dong or Min River but could be derived from other rivers draining similar rocks as those now found in these modern basins and which are common across southern China.

The indication is that across the central PRMB we see local or restricted sediment derivation throughout the Eocene-Oligocene. If there was a paleo-Pearl River at that time it must have been small and did not extend further into southern China than the modern Bei or Dong Rivers. Sources in Indochina or further west in the modern PRD can be firmly excluded (Fig. 7 and 11).

Previous studies instead argue for a greater change of provenance between the Oligocene and Miocene (Clift et al., 2002a; Liu et al., 2016; Shao et al., 2013; Tang et al., 2004). This interpretation is consistent with heavy mineral and clay mineral analysis (Shao et al., 2013; Tang et al., 2004). A rapid change in bulk sediment Nd isotope values after 23 Ma

733 towards the modern average (Clift et al., 2002a) argues for a widening of the basin towards
734 the modern configuration after that time.

735 Shao *et al* (2016; 2015) argued that the paleo-Pearl River enlarged its catchment area
736 during the late Oligocene, involving a migration of the headwaters towards the west of the
737 Cathaysia Block. Such a migration is not required in light of our better understanding of
738 source diversity in this study. Our work also calls in question the southerly provenance of
739 Upper Oligocene sediments to Well L-21 inferred by Shao *et al*. (2015). They argued that
740 Neoproterozoic zircons in those deposits were not sourced from South China because the
741 900–1100 Ma age grouping they found were not present in recent sediments from the PRMB.
742 Our work now shows that the Bei River contains such grains and a restricted river flowing
743 from the north can explain this spectrum with the need for flow from the south. In contrast, if
744 the structural high to the south of Well-21 contained source rocks with such old grains then
745 we might almost expect to see them in significant numbers at IODP Site U1435, whereas
746 they actually comprise <2% of the entire U1435 dataset.

747

748 **Conclusions**

749 In this study we present a series of bulk sediment geochemical analyses from
750 sediments taken from the different tributaries of the Pearl River and supplement these with
751 single grain U-Pb dating of zircon grains from the same samples in order to determine what is
752 controlling the patterns of erosion in the modern drainage system. The Chemical Index of
753 Alteration shows that the degree of weathering decreases downstream from the headwaters.
754 We interpret this to reflect the progressive removal of altered, fine-grained material so that
755 the sand close to the river mouth is relatively quartz rich and less weathered than proximal
756 sediments that have experienced strong subtropical weathering in the headwaters. Sr and Nd

757 isotopes can be used to constrain provenance. The general correlation of Sr and Nd, with the
758 exception of one sample from the Liu River, suggests that Sr is also largely provenance-
759 driven. Examination of how these isotopes changed downstream highlights the importance of
760 sediment supply from the Hongshui and Yu Rivers and indicates that the Gui, Liu and Dong
761 Rivers in particular are weak contributors of sediment to the mainstream. A progressive shift
762 towards more negative ε_{Nd} values close to the River mouth cannot only be explained by flux
763 from the Bei River.

764 Zircon U-Pb data are broadly consistent with the above results and confirm that the
765 Gui and Liu Rivers, which drained from the north towards the mainstream in the modern
766 catchment are relatively weak contributors of sediment. Zircon ages also support strong
767 sediment derivation from the Bei River. Zircon populations in the Dong River are quite
768 similar to those from a previously characterized sediment (R11) close to the river mouth,
769 although the present geometry precludes a direct connection between the systems. It is not
770 entirely clear whether R11 is a good representation of net flux to South China Sea because its
771 character is inconsistent with many of the samples analyzed in this study since it indicates
772 sources close to those of the Dong River, with which it has no confluence. The zircon data
773 does however emphasize the importance of the Hongshui and Yu Rivers in supplying
774 sediment to the mainstream. The role of the Dong River is not well defined, but Nd isotopes
775 suggest that it is not important.

776 Within the western part of the catchment erosion appears to be concentrated in the
777 highest topographic regions, the headwaters of the Hongshui River, that are also
778 characterized by the steepest slopes and greatest occurrence of earthquakes and rock uplift.
779 We infer that tectonic processes dominate in controlling erosion across the Pearl River
780 drainage. Precipitation is a secondary control because this is stronger in the eastern part of the
781 basin, whereas sediment supply is dominantly from the headwaters in the far West.

Comparison of the modern river with sediments from IODP Site U1435 show that these are quite different from the lower reaches of the modern river, but are similar to the Dong River. Zircon age populations show a relatively simple structure spanning 60–170 Ma, suggestive of a local source within the Cathaysia basement of southern China or even within the PRMB. Only the oldest sediment at this site shows any difference, with a greater diversity of ages (some 200–300 Ma grains), which implies a restricted regional river, not on the scale of the modern system. The closest similarity would be the modern Dong River draining eastern Cathaysia. Our results rule out the presence of sediment supply from Indochina during the Eocene and can be most easily explained in terms of drainage either from local tectonic blocks within the PRMB or the immediately adjacent segments of southern China.

Comparison of our results with Eocene and Oligocene sediments in the PRMB previously analyzed for zircon show close similarity, indicating a coherent drainage system with a much more restricted catchment than seen in the present day. Some of the sites appear to show local derivation but others can be explained by a river similar to the modern Dong system. Suggestions that the presence of Neoproterozoic grains in the Upper Oligocene within the PRMB imply sediment flux from the South appeared to be in error, as these can be supplied from a simple river comparable to the modern Bei River. We caution against using simple comparison with bedrock values in interpreting provenance data but emphasize the importance of comparison with the modern river system when interpreting ancient sedimentary rocks in the South China offshore area.

Acknowledgements

PDC thanks USSSP for financial support to the project, as well as additional funds from the Charles T. McCord Chair in Petroleum Geology at Louisiana State University. PB and KP

806 acknowledge financial support through the Max Planck Institute for Marine Microbiology
807 (Bremen) and the Institute for Chemistry and Biology of the Marine Environment (ICBM,
808 Oldenburg). We wish to thank Fuyuan Wu from the Chinese Academy of Sciences, Beijing
809 and Martina Schulz from ICBM (Oldenburg) for their help in making this project possible.
810 PB and KP thank the Max Planck Institute for Marine Microbiology (Bremen) and the ICBM
811 (University of Oldenburg) for financial support.

812

813

Figure Captions

Figure 1. A) Map showing the Pearl River area in a regional context, as well as the location of IODP Site U1435, ODP Site 1148 and industrial wells. B) Close-up image of the distributary system in the Pearl River Mouth area. C) Map showing the distribution of the Pearl River tributaries, as well as the sampling locations.

Figure 2. Map showing the major tectonic blocks within the Pearl River catchment, as well as the sample locations. Cathaysia block covers the SE area from which most our samples were derived. The Yangtze block includes only three of the samples in the NE of catchment. The boundary between these two blocks is modified after He et al. (2014). Subdivisions within these blocks are defined based on the results of the analysis presented here.

Figure 3. Geological map of the Pearl River catchment modified from the China Geological Map (2010). The western part mostly consists of carbonate from Paleozoic and Triassic age with much smaller amounts of clastic sedimentary rocks. The eastern part shows a wide distribution of igneous rocks together with Mesozoic sedimentary rocks.

Figure 4. Sedimentary log of the section drilled at IODP Site U1435 showing the section sampled for U-Pb zircon dating as part of this study. Sample points are marked by arrows. Modified after Li et al. (2015b).

Figure 5. Geochemical signature of the analyzed samples illustrated by a CN-A-K ternary diagram (Fedo et al., 1995), constructed using the mole weight of Na_2O and CaO* (CaO* represent the CaO associated with silicate, excluding all the carbonate) Al_2O_3 and K_2O respectively. Samples closer to Al_2O_3 are rich in kaolinite, chlorite and/or gibbsite (representing by Kao, Chl and Gib). CIA values is also calculated and shown on the left side, with its values are correlated with the CN-A-K. Sample P1, from the east of the Pearl River catchment area, has the lowest value of CIA and indicates high contents of K_2O and biotite. Abbreviations: sm (smectite), pl (plagioclase), ksp (K-feldspar), il (illite), m (muscovite).

Figure 6. Cross plot of $^{87}Sr/^{86}Sr$ and ε_{Nd} values for modern Pearl River samples in this study compared with results from generally finer grained sediments from the same river by Liu et al. (2007), as well as Holocene sediments from the Pearl River delta by Hu et al. (2013).

Figure 7. Kernel density estimation (KDE) plots of detrital zircon ages from IODP Site U1435, from select wells from the Pearl River Mouth Basin from Shao et al. (2016) and from the Pearl River tributaries. Min River sediment data is from Xu et al. (2016). Bedrock ages from Cathaysia and the western and southeastern Yangtze Blocks are also compared, from compilation of He et al. (2014). Patterned vertical bars represent identified discrete ages populations discussed in the text.

Figure 8. Principal Component Analysis (PCA) plots for major element compositions A) of the modern Pearl River samples, and B) compared with upper crustal average from Rudnick and Fountain (1995). Note general similarity of the samples with the possible exception of P1 (Dong River).

Figure 9. A) $^{87}Sr/^{86}Sr$ and B) ε_{Nd} values are plotted showing the downstream evolution. A) Most of the detrital sediments have similar values between 0.72 and 0.74. Sample 105 (Liu River) and sample 501 (Gui River) show much higher values of $^{87}Sr/^{86}Sr$ than most of the tributaries. Sample 906 (SW Yu River) has a smaller value, suggesting that none of these rivers are large contributors. B) ε_{Nd} is more variable than $^{87}Sr/^{86}Sr$. Sample 501 (Gui River) is the most negative at around -15. Sample 206, which represent all the tributaries from the NW Liu and Hongshui Rivers, has the most positive value around -8.5.

Figure 10. Multidimensional Scaling (MDS) plot of all the zircon age from IODP Site U1435, the Pearl River tributaries, Pearl River Mouth Basin drill cores and possible bedrock source blocks. Pearl River Mouth Basin data are from Shao et al. (2016). Min River sediment data is from Xu et al. (2016). Bedrock ages from Cathaysia and the western and southeastern Yangtze Blocks are also compared, from compilation of He et al. (2014).

Figure 11. Pie charts representing the general structure of the detrital zircon age assemblages plotted against the stream flow direction. Arrow on the right indicates the direction downstream. P7 represents the most downstream sample on the mainstream. Sample 005 shows the greatest similarity to P7, suggesting that the Hongshui could be the greatest sediment net contributor to the net flow.

Figure 12. Average annual precipitation for the Yangtze River Basin calculated from calibrated, satellite-derived rainfall (product TRMM 2B31). See Bookhagen and Burbank (2010) for processing details.

885 Table 1. River sediment sample list with their locations, sedimentary types and tributary
886 names within the Pearl River capture area.

887

888 Table 2. Bulk geochemistry result derived from XRF analysis. Major element contents are
889 given in weight percentage. Trace element concentrations are in ppm. CIA* is calculated
890 using the method of Singh et al.(2005).

891

892 Table S1. River sediment's zircon U-Pb dating age results derived by LA-ICP-MS.

893

894 Table S2. IODP Site U1435's zircon U-Pb dating age results from LA-ICP-MS.

895

References

Amidon, W.H., Burbank, D.W., Gehrels, G.E., 2005. U-Pb zircon ages as a sediment mixing tracer in the Nepal Himalaya. Earth and Planetary Science Letters, 235(1-2): 244-260.

Black, L.P., Kamo, S.L., Allen, C.M., Aleinikoff, J.N., Davis, D.W., Korsch, R.J., Foudoulis, C., 2003. TEMORA 1: a new zircon standard for Phanerozoic U-Pb geochronology. Chemical Geology, 200: 155–170.

Bookhagen, B., Burbank, D.W., 2010. Towards a complete Himalayan hydrological budget: The spatiotemporal distribution of snow melt and rainfall and their impact on river discharge. Journal of Geophysical Research. doi:10.1029/2009jf001426.

Bookhagen, B., Strecker, M.R., 2012. Spatiotemporal trends in erosion rates across a pronounced rainfall gradient: Examples from the southern Central Andes. Earth and Planetary Science Letters, 327-328: 97–110. 10.1016/j.epsl.2012.02.005.

Bookhagen, B., Thiede, R., Draganits, E., Grasemann, B., Haselton, K., Janda, C., Sobel, E.R., Strecker, M.R., 2001. Tectonic uplift and climatic factors controlling erosion along the southern Himalayan front. Journal of Asian Earth Sciences, 19(3A): 6-7.

Briais, A., Patriat, P., Tapponnier, P., 1993. Updated interpretation of magnetic anomalies and seafloor spreading stages in the South China Sea: implications for the Tertiary tectonics of Southeast Asia. Journal of Geophysical Research, 98: 6299-6328. doi:10.1029/92JB02280.

Brookfield, M.E., 1998. The evolution of the great river systems of southern Asia during the Cenozoic India-Asia collision; rivers draining southwards. Geomorphology, 22(3-4): 285-312.

Burbank, D.W., Blythe, A.E., Putkonen, J., Pratt-Sitaula, B., Gabet, E., Oskins, M., Barros, A., Ojha, T.P., 2003. Decoupling of erosion and precipitation in the Himalayas. Nature, 426: 652–655.

Carter, A., Bristow, C.S., 2001. Detrital zircon geochronology: enhancing the quality of sedimentary source information through improved methodology and combined U–Pb and fission-track techniques. Basin Research, 12(1): 47-57. doi: 0.1046/j.1365-2117.2000.00112.

Carter, A., Roques, D., Bristow, C., Kinny, P.D., 2001. Understanding Mesozoic accretion in Southeast Asia: Significance of Triassic thermotectonism (Indosinian orogeny) in Vietnam. Geology, 29: 211–214.

Chen, S.Z., Pei, C.M., 1993. Geology and geochemistry of source rocks of the eastern Pearl River mouth Basin, South China sea. J. SE Asian Earth Sci, 8: 393-406.

Chen, Z., Burchfiel, B.C., Liu, Y., King, R.W., Royden, L.H., Tang, W., Wang, E., Zhao, J., Zhang, X., 2000. Global positioning system measurements from eastern Tibet and their implications for India/Eurasia intercontinental deformation. Journal of Geophysical Research, 105(B7): 16,215-16,227.

Chinese Geology Survey, 2010. China Geology Map. Chinese Geology Survey, Beijing, China.

Clark, M.K., Schoenbohm, L.M., Royden, L.H., Whipple, K.X., Burchfiel, B.C., Zhang, X., Tang, W., Wang, E., Chen, L., 2004. Surface uplift, tectonics, and erosion of eastern Tibet from large-scale drainage patterns. Tectonics, 23, TC1006. doi:10.1029/2002TC001402.

Clift, P., Lee, J.I., Clark, M.K., Blusztajn, J., 2002a. Erosional response of South China to arc rifting and monsoonal strengthening; a record from the South China Sea. Marine Geology, 184(3–4): 207-226. doi:10.1016/S0025-3227(01)00301-2.

943 Clift, P., Lin, J., Barckhausen, U., 2002b. Evidence of low flexural rigidity and low viscosity
944 lower continental crust during continental break-up in the South China Sea. Marine
945 and Petroleum Geology, 19(8): 951-970.
946 Clift, P.D., 2016. Assessing effective provenance methods for fluvial sediment in the South
947 China Sea. In: Clift, P.D., Harff, J., Wu, J., Qui, Y. (Eds.), River-dominated shelf
948 sediments of East Asian seas, 429, Geological Society of London, London,
949 doi:10.1144/SP429.3.
950 Clift, P.D., Blusztajn, J., Nguyen, D.A., 2006. Large-scale drainage capture and surface uplift
951 in eastern Tibet-SW China before 24 Ma inferred from sediments of the Hanoi Basin,
952 Vietnam. Geophysical Research Letters, 33(L19403). doi:10.1029/2006GL027772.
953 Clift, P.D., Giosan, L., 2014. Sediment fluxes and buffering in the post-glacial Indus Basin.
954 Basin Research, 25: 1–18. doi: 10.1111/bre.12038.
955 Compston, W., Williams, I.S., Kirschvink, J.L., Zhang, Z., Ma, G., 1992. Zircon U–Pb ages
956 for the Early Cambrian time-scale. J. Geol. Soc. Lond, 149,: 171–184.
957 Cullen, A., Reemst, P., Henstra, G., Gozzard, S., Ray, A., 2010. Rifting of the South China
958 Sea: new perspectives. Petroleum Geoscience, 16: 273–282.
959 Derry, L.A., France-Lanord, C., 1996. Neogene Himalayan weathering history and river
960 $^{87}Sr/^{86}Sr$; impact on the marine Sr record. Earth and Planetary Science Letters, 142:
961 59-74.
962 Ekström, G., Nettles, M., Dziewonski, A.M., 2012. The global CMT project 2004-2010:
963 Centroid-moment tensors for 13,017 earthquakes. Physics of the Earth and Planetary
964 Interiors, 200-201: 1-9. doi:10.1016/j.pepi.2012.04.002.
965 Fedo, C.M., Nesbitt, H.W., Young, G.M., 1995. Unraveling the effects of potassium
966 metasomatism in sedimentary rocks and paleosols, with implications for
967 paleoweathering conditions and provenance. Geology, 23: 921–924.
968 Garçon, M., Chauvel, C., France-Lanord, C., Huyghe, P., Lavé, J., 2013. Continental
969 sedimentary processes decouple Nd and Hf isotopes. Geochimica et Cosmochimica
970 Acta, 121: 177-195.
971 Garçon, M., Chauvel, C., France-Lanord, C., Limonta, M., Garzanti, E., 2014. Which
972 minerals control the Nd–Hf–Sr–Pb isotopic compositions of river sediments?
973 Chemical Geology, 364: 42–55. doi:10.1016/j.chemgeo.2013.11.018.
974 Gawthorpe, R.L., Leeder, M.R., 2000. Tectono-sedimentary evolution of active extensional
975 basins. Basin Research, 12(3-4): 195-218.
976 Gehrels, G.E., 2014. Detrital Zircon U-Pb Geochronology Applied to Tectonics. Annual
977 Review of Earth and Planetary Sciences, 42: 127-149. DOI: 10.1146/annurev-earth-
978 050212-124012.
979 Goldstein, S.L., O'Nions, R.K., Hamilton, P.J., 1984. A Sm-Nd isotopic study of atmospheric
980 dusts and particulates from major river systems. Earth and Planetary Science Letters,
981 70(2): 221-236.
982 He, M., Zheng, H., Bookhagen, B., Clift, P.D., 2014. Controls on erosion intensity in the
983 Yangtze River basin tracked by U-Pb detrital zircon dating. Earth Science Reviews,
984 136: 121–140. doi:10.1016/j.earscirev.2014.05.014.
985 He, M., Zheng, H., Clift, P.D., 2013. Zircon U–Pb geochronology and Hf isotope data from
986 the Yangtze River sands: Implications for major magmatic events and crustal
987 evolution in Central China. Chemical Geology, 360-361: 186-203.
988 Hillier, S., 1995. Erosion, sedimentation, and sedimentary origin of clays. In: Velde, B. (Ed.),
989 Clays and the environment, Springer Verlag, Berlin, pp. 162-219,
990 Hodges, K., 2003. Geochronology and thermochronology in orogenic systems. In: Rudnick,
991 R. (Ed.), The Crust, Elsevier-Science, Amsterdam, pp. 263-292,

992 Hu, D., Clift, P.D., Böning, P., Hannigan, R., Hillier, S., Blusztajn, J., Wang, S., Fuller, D.Q.,
993 2013. Holocene evolution in weathering and erosion patterns in the Pearl River delta.
994 Geochemistry Geophysics Geosystems, 14. doi:10.1002/ggge.20166.
995 Jackson, S.E., Pearson, N.J., Griffin, W.L., Belousova, E.A., 2004. The application of laser
996 ablation-inductively coupled plasma-mass spectrometry (LA-ICP-MS) to in situ U–Pb
997 zircon geochronology. Chemical Geology, 211: 47–69.
998 Jacobsen, S.B., Wasserburg, G.J., 1980. Sm-Nd isotopic evolution of chondrites. Earth and
999 Planetary Science Letters 50(1): 139-155.
1000 Jahn, B.M., Zhou, X.H., Li, J.L., 1990. Formation and tectonic evolution of Southeastern
1001 China and Taiwan: Isotopic and geochemical constraints. Tectonophysics, 183: 145-
1002 160.
1003 Jochum, K.P., Weis, U., Stoll, B., Kuzmin, D., Yang, Q., Raczek, I., Jacob, D.E., Stracke, A.,
1004 Birbaum, K., Frick, D.A., Günther, D., Enzweiler, J., 2011. Determination of
1005 Reference Values for NIST SRM 610–617 Glasses Following ISO Guidelines.
1006 Geostandards and Geoanalytical Research, 35: 397–429. doi: 10.1111/j.1751-
1007 908X.2011.00120.x.
1008 Kusky, T.M., Windley, B.F., Zhai, M.-G., 2007. Tectonic evolution of the North China Block:
1009 from orogen to craton to orogen. In: Zhai, M.G., Windley, B.F., Kusky, T.M., Meng,
1010 Q.R. (Eds.), Mesozoic Sub-Continental Lithospheric Thinning Under Eastern Asia.
1011 Special Publication, 280, Geological Society, London, pp. 1-34, doi:
1012 10.1144/SP280.1.
1013 Lan, Q., Yan, Y., Huang, C.-Y., Clift, P.D., Li, X., Chen, W., Zhang, X., Yu, M., 2014.
1014 Tectonics, topography, and river system transition in East Tibet: Insights from the
1015 sedimentary record in Taiwan. Geochemistry, Geophysics, Geosystems, 15(9): 3658-
1016 3674. 10.1002/2014GC005310.
1017 Lepvrier, C., Maluski, H., Vu, V.T., Leyreloup, A., Phan, T.T., Vuong, N.V., 2004. The
1018 Early Triassic Indosinian orogeny in Vietnam (Truong Son Belt and Kontum Massif);
1019 implications for the geodynamic evolution of Indochina. Tectonophysics, 393: 87-118.
1020 Li, C.-F., Lin, J., Kulhanek, D.K., Expedition 349 Scientists, 2015a. Proceedings of the
1021 International Ocean Discovery Program, 349: South China Sea Tectonics,
1022 International Ocean Discovery Program, College Station, TX.
1023 Li, C.-F., Lin, J., Kulhanek, D.K. et al., 2015b. Site U1435. Proceedings of the International
1024 Ocean Discovery Program, 349. doi:10.14379/iodp.proc.349.105.2015.
1025 Li, C.-F., Xu, X., Expedition 349 Scientific Party, 2014. Ages and magnetic structures of the
1026 South China Sea constrained by deep tow magnetic surveys and IODP Expedition 349.
1027 Geochemistry, Geophysics, Geosystems, 15: 4958–4983. doi:10.1002/
1028 2014GC005567.
1029 Li, X.-H., Wei, G., Shao, L., Liu, Y., Liang, X., Jian, Z., Sun, M., Wang, P., 2003.
1030 Geochemical and Nd isotopic variations in sediments of the South China Sea: a
1031 response to Cenozoic tectonism in SE Asia. Earth and Planetary Science Letters,
1032 211(3–4): 207-220. doi:10.1016/S0012-821X(03)00229-2.
1033 Li, X.H., 1997. Timing of Cathaysia block formation: constraints from SHRIMP U-Pb zircon
1034 geochronology. Episodes, 20: 188-192.
1035 Li, X.H., 1999. U-Pb zircon ages of granites from the southern margin of the Yangtze Block;
1036 timing of Neoproterozoic Jinning; orogeny in SE China and implications for Rodinia
1037 assembly. Precambrian Research, 97: 43–57.
1038 Liu, Q., Zhu, H., Shu, Y., Zhu, X., Yang, X., Chen, L., Tan, M., Geng, M., 2016. Provenance
1039 identification and sedimentary analysis of the beach and bar systems in the
1040 Palaeogene of the Enping Sag, Pearl River Mouth Basin, South China Sea. Marine
1041 and Petroleum Geology, 70: 251-272.

Liu, Y., Gao, S., Hu, Z., Gao, C., Zong, K., Wang, D., 2010. Continental and Oceanic Crust Recycling-induced Melt–Peridotite Interactions in the Trans-North China Orogen: U–Pb Dating, Hf Isotopes and Trace Elements in Zircons from Mantle Xenoliths. Journal of Petrology, 51(1-2): 537-571. 10.1093/petrology/egp082.

Liu, Y., Hu, Z., Gao, S., Günther, D., Xu, J., Gao, C., Chen, H., 2008. In situ analysis of major and trace elements of anhydrous minerals by LA-ICP-MS without applying an internal standard. Chemical Geology, 257(1–2): 34-43. doi:10.1016/j.chemgeo.2008.08.004.

Liu, Z., Colin, C., Huang, W., Le, K.P., Tong, S., Chen, Z., Trentesaux, A., 2007. Climatic and tectonic controls on weathering in south China and Indochina Peninsula: Clay mineralogical and geochemical investigations from the Pearl, Red, and Mekong drainage basins. Geochemistry Geophysics Geosystems, 8, Q05005. doi:10.1029/2006GC001490.

Malusà, M.G., Resentini, A., Garzanti, E., 2016. Hydraulic sorting and mineral fertility bias in detrital geochronology. Gondwana Research, 31: 1-19. doi:10.1016/j.gr.2015.09.002.

Meinhardt, A.K., Pahnke, K., Böning, P., Schnetger, B., Brumsack, H.J., 2016. Climate change and response in bottom water circulation and sediment provenance in the Central Arctic Ocean since the Last Glacial. Chemical Geology, 427: 98-108. doi:10.1016/j.chemgeo.2016.02.019.

Milliman, J.D., Meade, R.H., 1983. World-wide delivery of sediment to the oceans. Journal of Geology, 91: 1–21.

Nesbitt, H.W., Young, G.M., 1982. Early Proterozoic climates and plate motions inferred from major element chemistry of lutites. Nature, 299(5885): 715-717.

Pubellier, M., Chamot-Rooke, N., Ego, F., Guezou, J.C., Konstantinovskaya, E., Rabaute, A., Ringenbach, J.C., 2008. Structural Map of Eastern Eurasia. Commission for the Geological Map of the World.

Raczek, I., Jochum, K.P., Hofmann, A.W., 2003. Neodymium and Strontium Isotope Data for USGS Reference Materials BCR-1, BCR-2, BHVO-1, BHVO-2, AGV-1, AGV-2, GSP-1, GSP-2 and Eight MPI-DING Reference Glasses. Geostandards Newsletter, 27(2): 173–179. doi;10.1111/j.1751-908X.2003.tb00644.x.

Resentini, A., Malusà, M.G., Garzanti, E., 2013. MinSORTING: An Excel® worksheet for modelling mineral grain-size distribution in sediments, with application to detrital geochronology and provenance studies. Computers & Geosciences, 59: 90-97. doi:10.1016/j.cageo.2013.05.015.

Rudnick, R.L., Fountain, D.M., 1995. Nature and composition of the continental crust; a lower crustal perspective. Reviews of Geophysics, 33: 267–309.

Sewell, R.J., Campbell, S.D.G., 1997. Geochemistry of coeval Mesozoic plutonic and volcanic suites in Hong Kong. Journal of the Geological Society, London, 154: 1053–1066.

Shao, L., Cao, L., Pang, X., Jiang, T., Qiao, P., Zhao, M., 2016. Detrital zircon provenance of the Paleogene syn-rift sediments in the northern South China Sea. Geochemistry, Geophysics, Geosystems, 17(2): 255-269. 10.1002/2015GC006113.

Shao, L., Pang, X., Qiao, P., 2008. Sedimentary filling of the Pearl River Mouth Basin and Its response to the evolution of the Pearl River. Acta Seismologica Sinica, 26(2): 179.

Shao, L., Qiao, P., Zhao, M., Li, Q., Wu, M., Pang, X., Zhang, H., 2015. Depositional characteristics of the northern South China Sea in response to the evolution of the Pearl River. Geological Society, London, Special Publications, 429. 10.1144/sp429.2.

Shao, L., Zhao, M., Qiao, P., 2013. The Characteristics of the sediment in Northern South China Sea and its response to the evolution of the Pearl River Journal of Quaternary Sciences, 33(4): 760-770.
Shipboard Scientific Party, 2000. Site 1148, Proceedings of the Ocean Drilling Program, Part A: Initial Reports.
Silverman, B.W., 1986. Density Estimation for Statistics and Data Analysis. Chapman and Hall, London, 176 pp.
Singh, S.K., Sarin, M.M., France-Lanord, C., 2005. Chemical erosion in the eastern Himalaya; major ion composition of the Brahmaputra and d13C of dissolved inorganic carbon. Geochimica et Cosmochimica Acta, 69(14): 3573-3588.
Sláma, J., Košler, J., Condon, D.J., Crowley, J.L., Gerdes, A., Hanchar, J.M., Horstwood, M.S.A., Morris, G.A., Nasdala, L., Norberg, N., Schaltegger, U., Schoene, B., Tubrett, M.N., Whitehouse, M.J., 2008. Plezovice zircon A new natural reference material for U–Pb and Hf isotopic microanalysis. Chemical Geology, 249: 1-35.
Suggate, S.M., Cottam, M.A., Hall, R., Sevastjanova, I., Forster, M.A., White, L.T., Armstrong, R.A., Carter, A., Mojares, E., 2014. South China continental margin signature for sandstones and granites from Palawan, Philippines. Gondwana Research, 26(2): 699-718. doi:10.1016/j.gr.2013.07.006.
Sun, W.H., Zhou, M.F., Gao, J.F., Yang, Y.H., Zhao, X.F., Zhao, J.H., 2009. Detrital zircon U–Pb geochronological and Lu–Hf isotopic constraints on the Precambrian magmatic and crustal evolution of the western Yangtze Block, SW China. Precambrian Research, 172: 99-126.
Tanaka, T., Togashi, S., Kamioka, H. et al., 2000. JNdi-1: a neodymium isotopic reference in consistency with LaJolla neodymium. Chemical Geology, 168: 279–281.
Tang, S., Shao, L., Zhao, Q., 2004. Characteristics of clay minerals in South China Sea since Oligocene and its significance. Acta Sedimentologica Sinica [in Chinese with English abstract], 22: 337–342.
Thirlwall, M.F., 1991. Long-term reproducibility of multicollector Sr and Nd isotope ratio analysis. Chemical Geology: Isotope Geoscience section, 94(2): 85-104.
Thiry, M., 2000. Palaeoclimatic interpretation of clay minerals in marine deposits; an outlook from the continental origin. Earth-Science Reviews, 49(1-4): 201-221.
Vermeesch, P., 2004. How many grains are needed for a provenance study? Earth and Planetary Science Letters, 224: 351–441.
Vermeesch, P., 2012. On the visualisation of detrital age distributions. Chemical Geology, 312–313: 190–194. doi:10.1016/j.chemgeo.2012.04.021.
Vermeesch, P., 2013. Multi-sample comparison of detrital age distributions. Chemical Geology, 341: 140–146. doi:10.1016/j.chemgeo.2013.01.010.
Vermeesch, P., Resentini, A., Garzanti, E., 2016. An R package for statistical provenance analysis. Sedimentary Geology, 336: 14-25. doi:10.1016/j.sedgeo.2016.01.009.
Wang, X.-L., Zhou, J.-C., Griffin, W.L., Wang, R.-C., Qiu, J.-S., O'Reilly, S.Y., Xu, X., Liu, X.-M., Zhang, G.-L., 2007. Detrital zircon geochronology of Precambrian basement sequences in the Jiangnan orogen: Dating the assembly of the Yangtze and Cathaysia Blocks. Precambrian Research, 159(1–2): 117-131. doi:10.1016/j.precamres.2007.06.005.
Wei, G., Liu, Y., Ma, J., Xie, L., Chen, J., Deng, W., Tang, S., 2012. Nd, Sr isotopes and elemental geochemistry of surface sediments from the South China Sea: Implications for Provenance Tracing. Marine Geology, 319–322: 21–34. doi:10.1016/j.margeo.2012.05.007.
Wiedenbeck, M., Allé, P., Corfu, F., Griffin, W.L., Meier, M., Oberli, F., Quadt, A.V., Roddick, J.C., Spiegel, W., 1995. Three natural zircon standards for U-Th-Pb, Lu-Hf

tarce element and REE analyses. Geostandards Newsletter, 19(1): 1-23. doi:10.1111/j.1751-908X.1995.tb00147.x.
Xu, Y., Wang, C.Y., Zhao, T., 2016. Using detrital zircons from river sands to constrain major tectono-thermal events of the Cathaysia Block, SE China. Journal of Asian Earth Sciences, 124: 1–13. doi:10.1016/j.jseaes.2016.04.012.
Yang, S., Zhang, F., Wang, Z., 2012. Grain size distribution and age population of detrital zircons from the Changjiang (Yangtze) River system, China. Chemical Geology, 296-297: 26-38.
Yao, Y., Zhan, W., Liu, Z., Zhang, Z., Zhan, M., Sun, J., 2013. Neotectonics and its Relations to the Evolution of the Pearl River Delta, Guangdong, China. Journal of Coastal Research, 66: 1-11.
Yu, Y., Zhang, C., Li, S., Zhu, R., Liu, J., Qin, C., Zhang, Z., 2015. Influences of Tibetan Plateau uplift on provenance evolution of the paleo-Pearl River. Chinese Journal of Geochemistry, 34(2): 208–218. doi:10.1007/s11631-015-0032-z.
Zhang, S., Liang, D., Gong, Z., Wu, K., Li, M., Song, F., Song, Z., Zhang, D., Wang, P., 2003. Geochemistry of petroleum systems in the eastern Pearl River Mouth Basin: evidence for mixed oils. Organic Geochemistry, 34(7): 971-991. doi:10.1016/S0146-6380(03)00034-2.
Zhang, W., Mu, S.-s., Zhang, Y.-j., Chen, K.-m., 2012. Seasonal and interannual variations of flow discharge from Pearl River into sea. Water Science and Engineering, 5(4): 399-409. doi:10.3882/j.issn.1674-2370.2012.04.004.
Zhao, M., Shao, L., Qiao, P., 2015. Characteristics of detrital zircon U-Pb geochronology of the Pearl River sands and its implication on provenances. Journal of Tongji University (Natural Sciences), 43(6): 915-923. doi:10.11908/j.issn.0253-374x.2015.06.018.
Zheng, H., Clift, P.D., Tada, R., Jia, J.T., He, M.Y., Wang, P., 2013. A Pre-Miocene Birth to the Yangtze River. Proceedings of the National Academy of Sciences: 1-6. doi:10.1073/pnas.1216241110.
Zhou, M.F., Yan, D.P., Kennedy, A.K., Li, Y., Ding, J., 2002. SHRIMP U-Pb zircon geochronological and geochemical evidence for Neoproterozoic arc-magmatism along the western margin of the Yangtze block, South China. Earth and Planetary Science Letters, 196: 51-67.
Zhu, W.L., Mi, L.J., 2010. Atlas of Oil and Gas Basins. Petroleum Industry Press China Sea (In Chinese): 102.

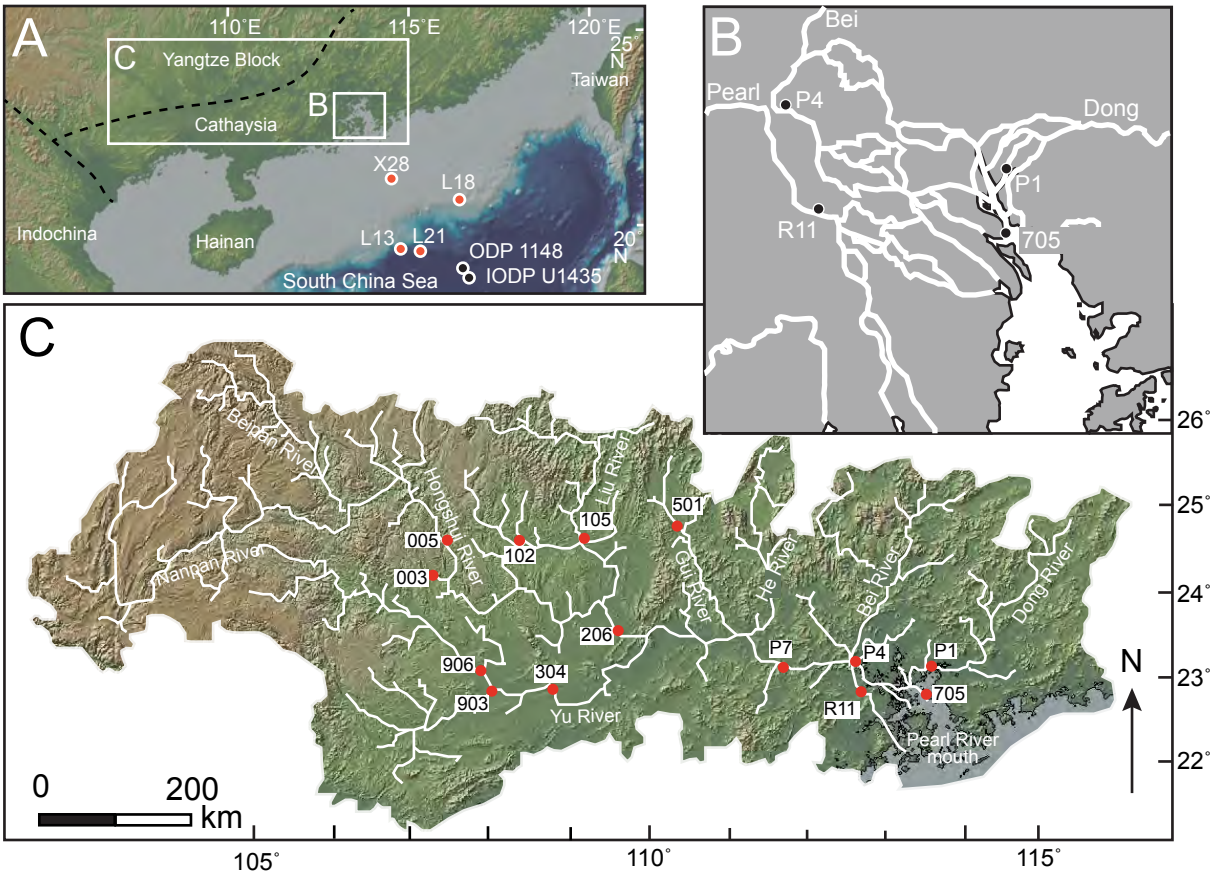

Figure 1
Liu et al

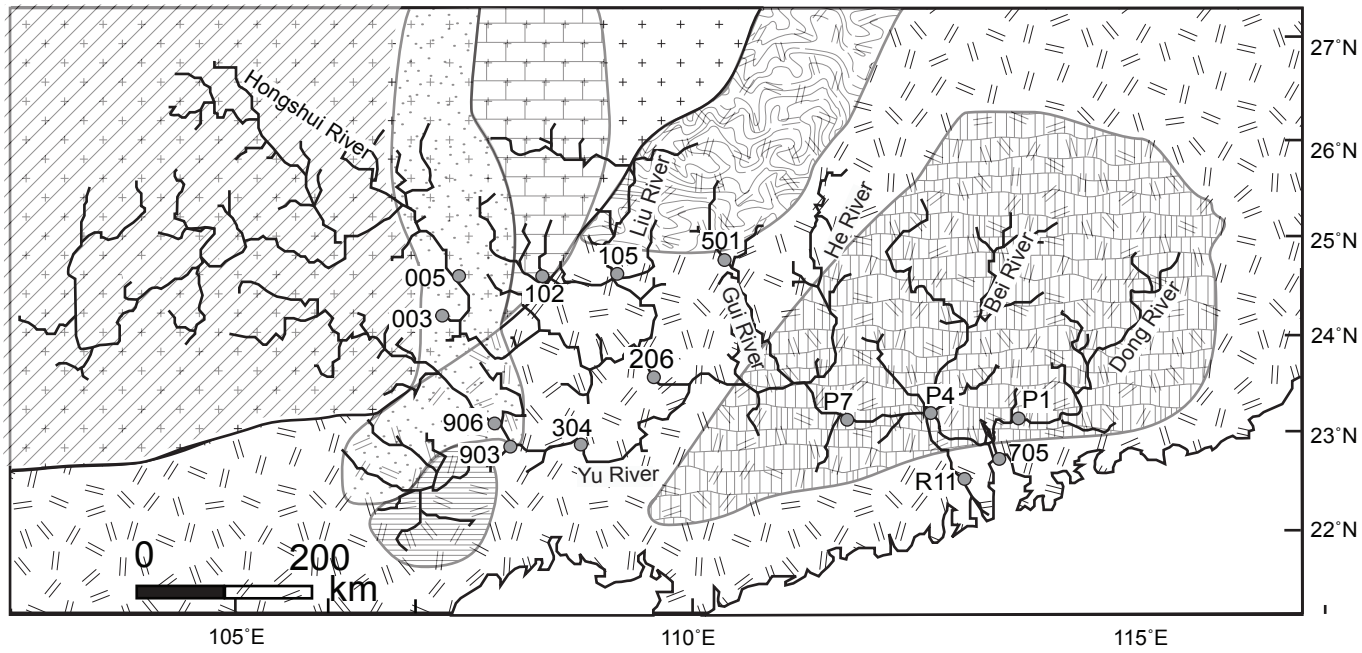

Yangtze Craton

Cathaysia

~100 Ma - Cretaceous arc influence

~250 Ma - Indosinian influence

~400 Ma - Caledonian influence

~800 Ma - Yangtze Craton influence

~1000 Ma - Cathaysia influence

~1800 Ma - Luliangian influence

Figure 2
Liu et al

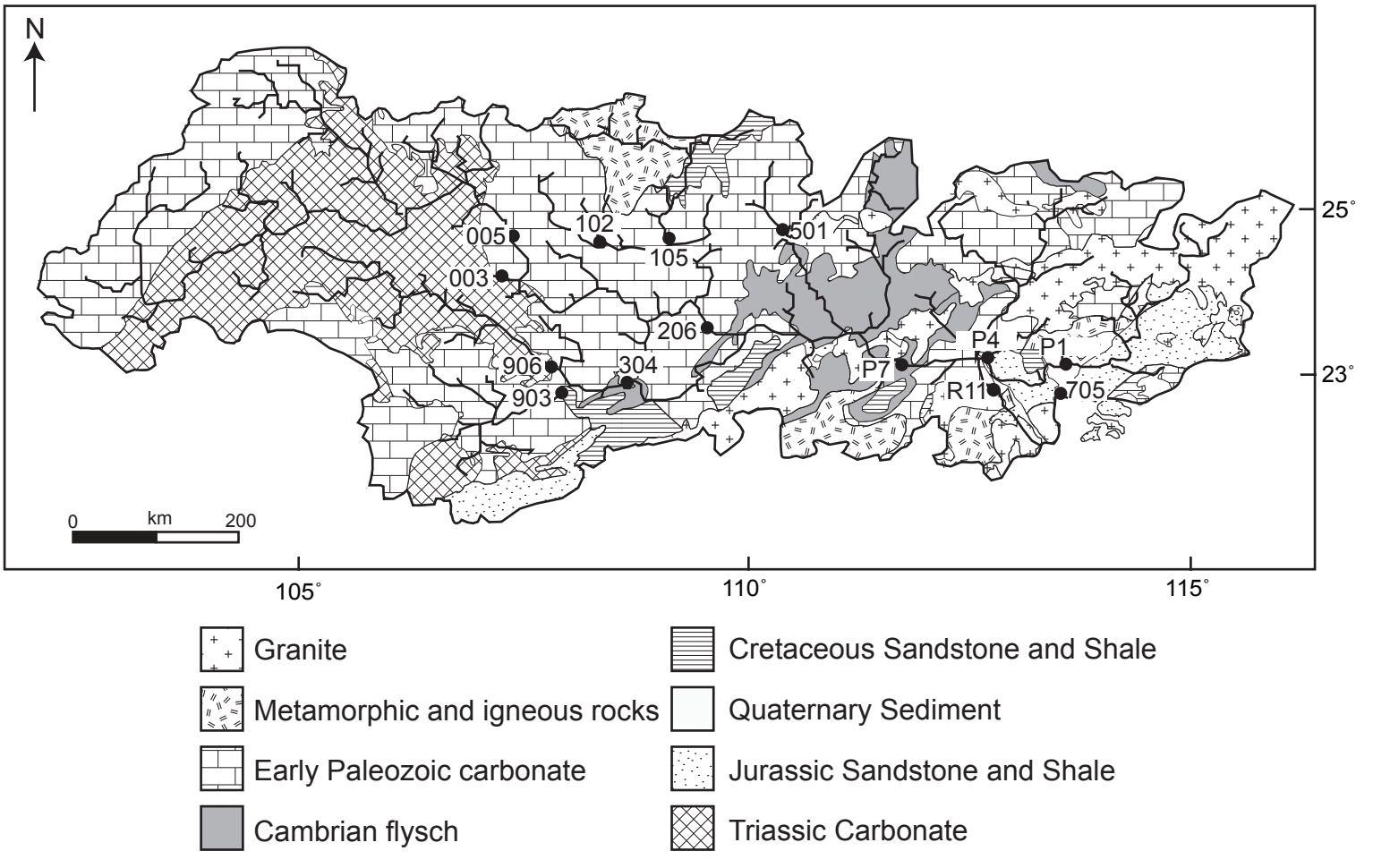

Figure 3
Liu et al

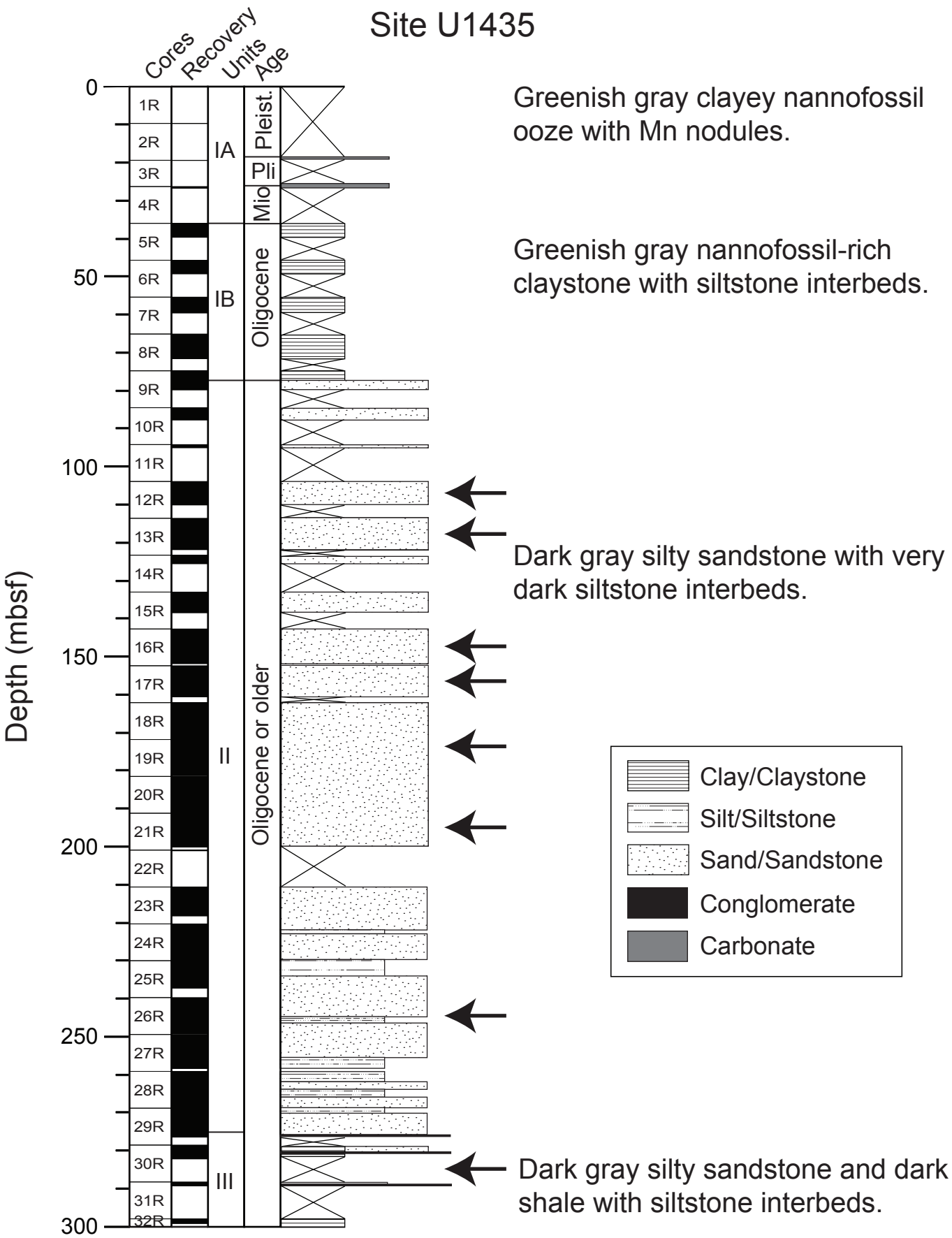

Figure 4
Liu et al.

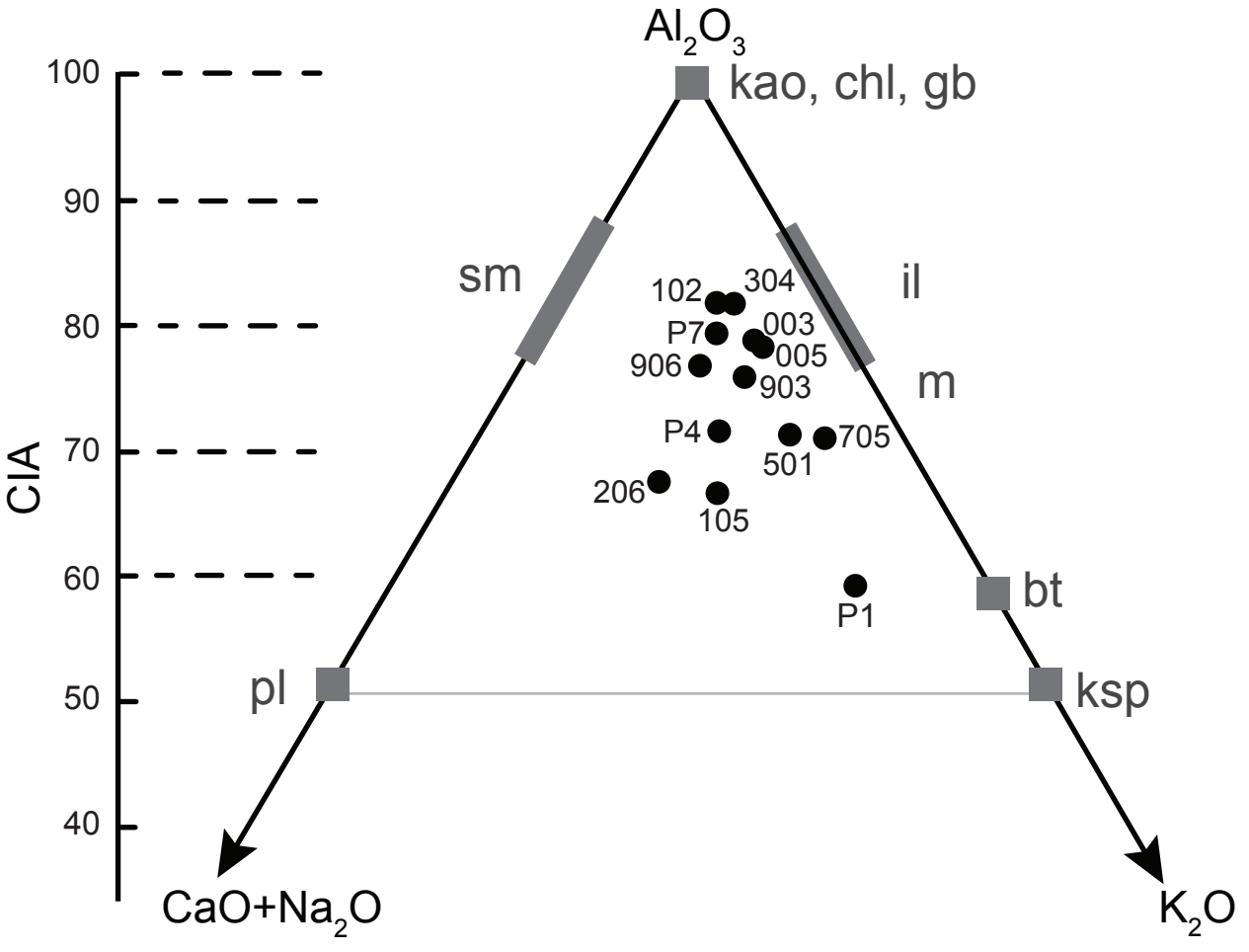

Figure 5
Liu et al

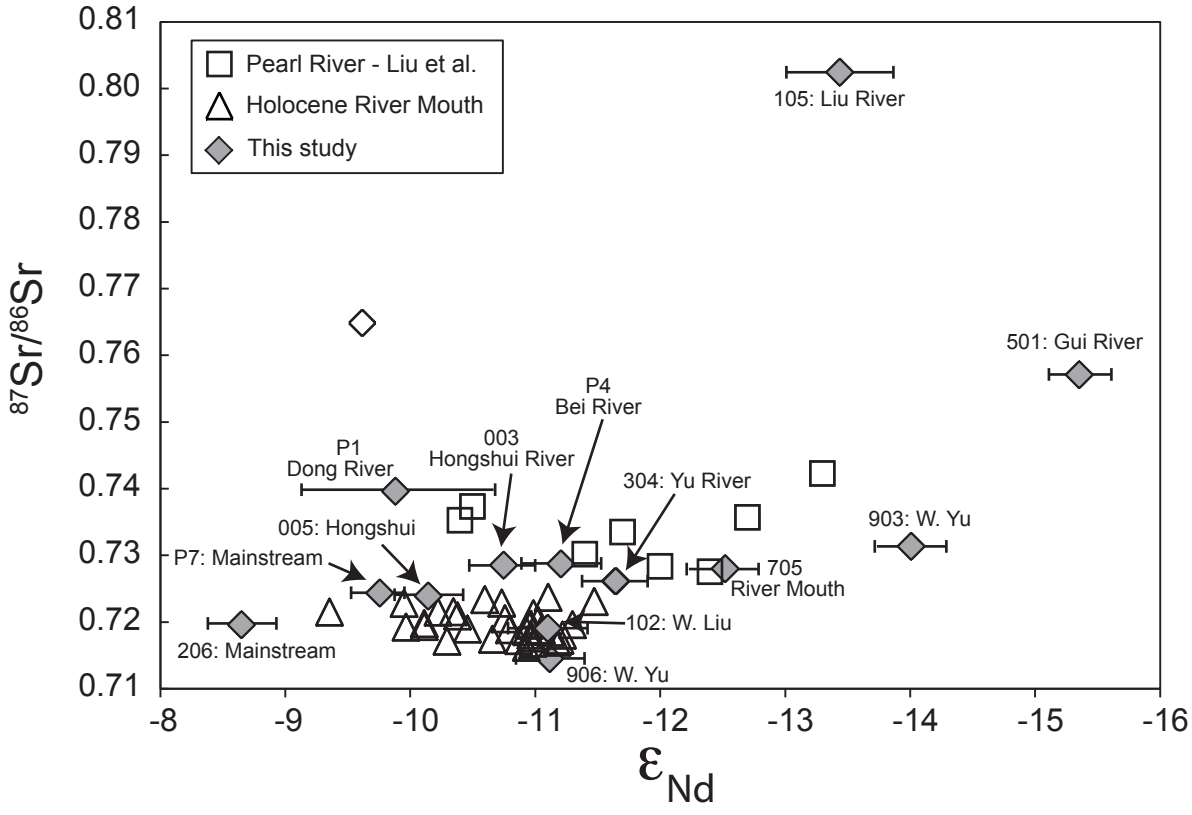

Figure 6
Liu et al

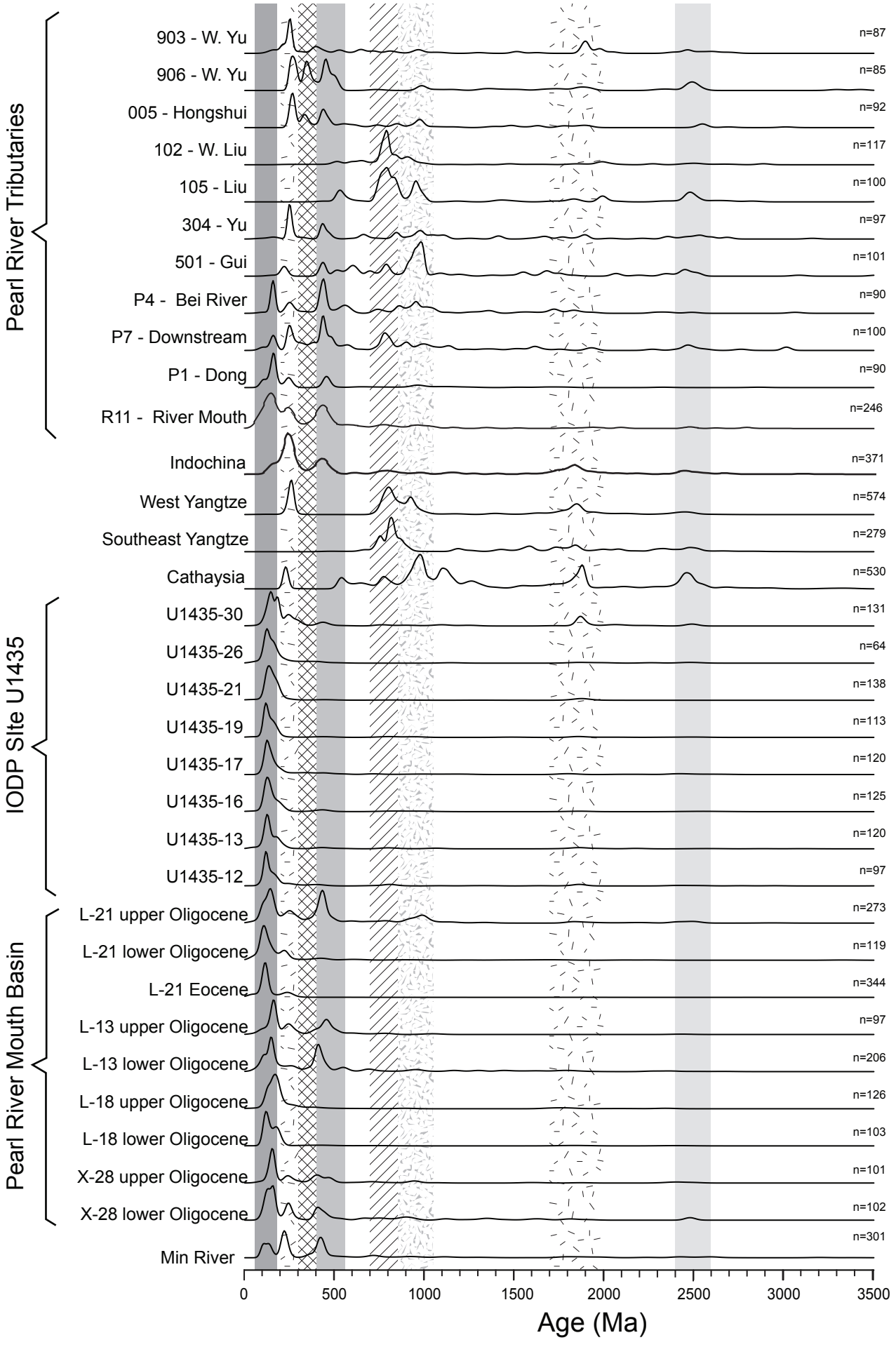

Figure 7
Liu et al

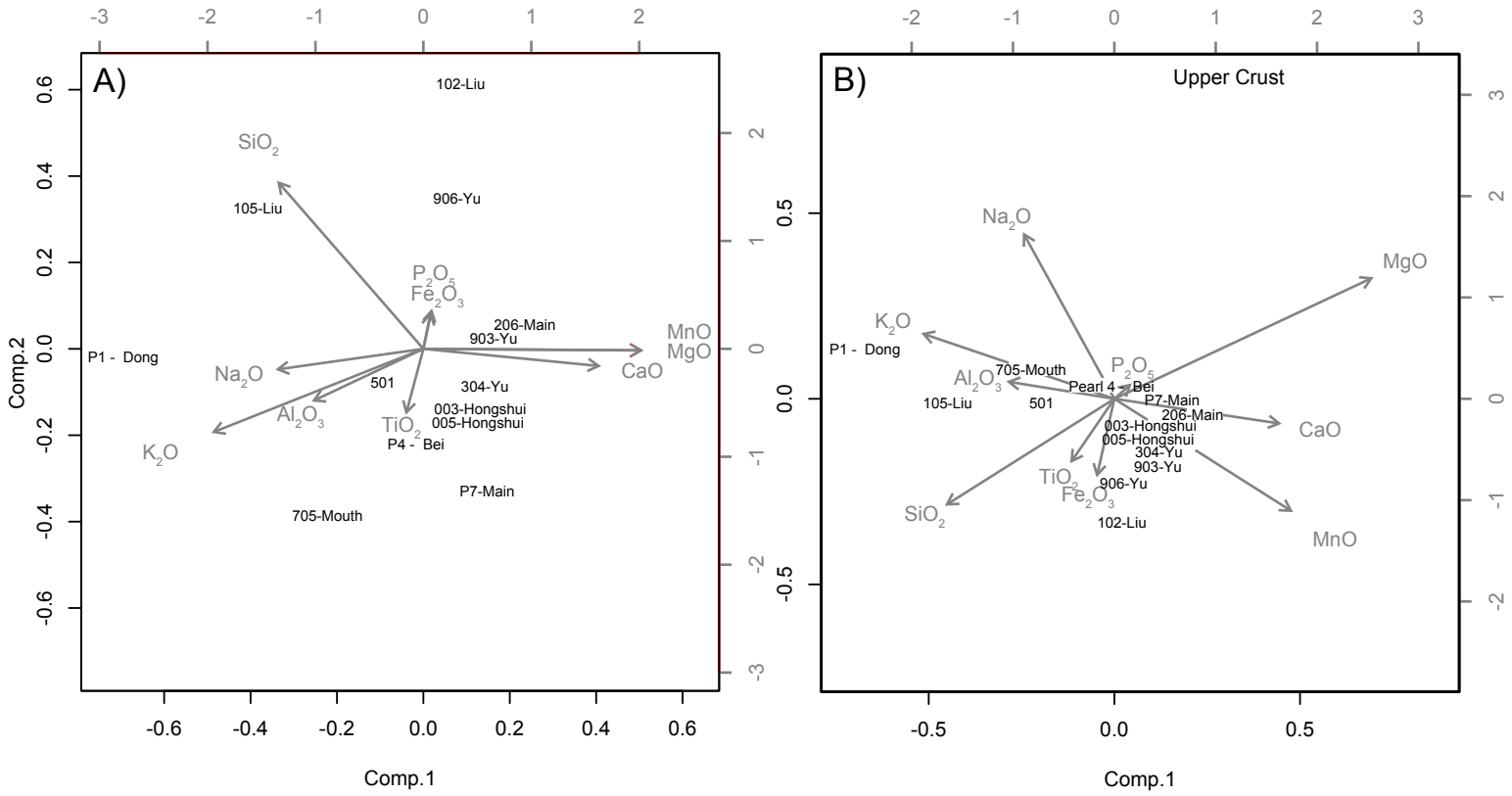

Figure 8
Liu et al.

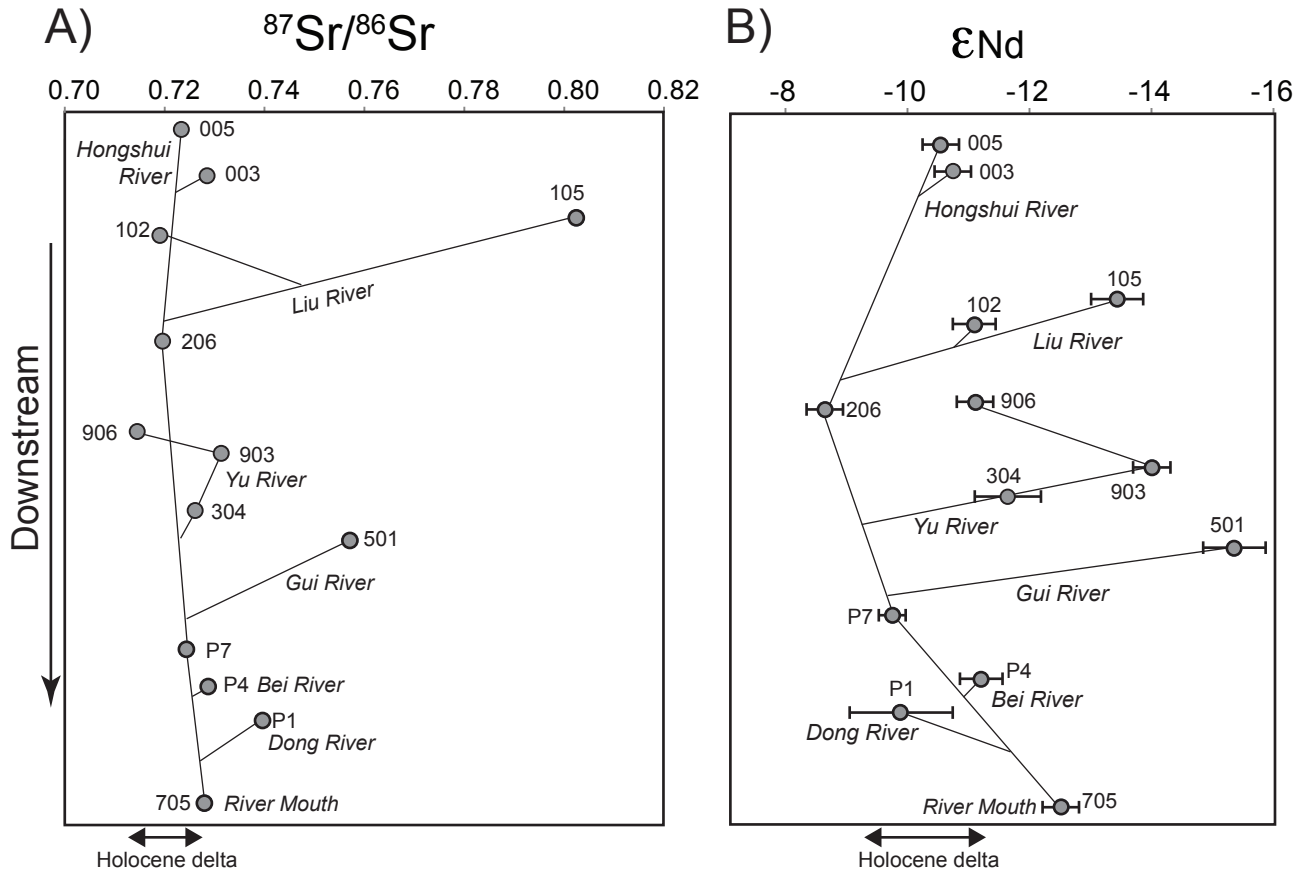

Figure 9
Liu et al

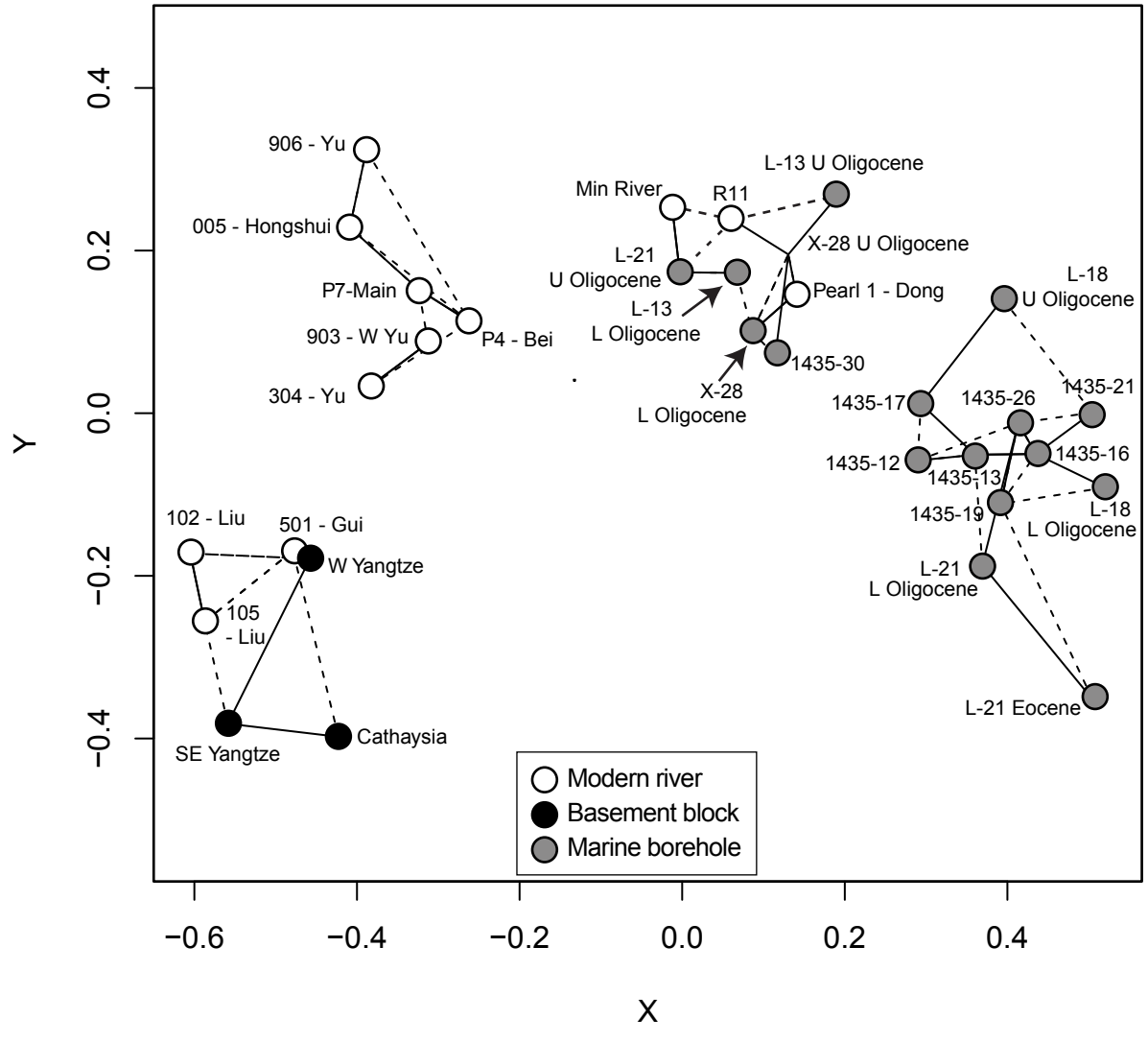

Figure 10
Liu et al

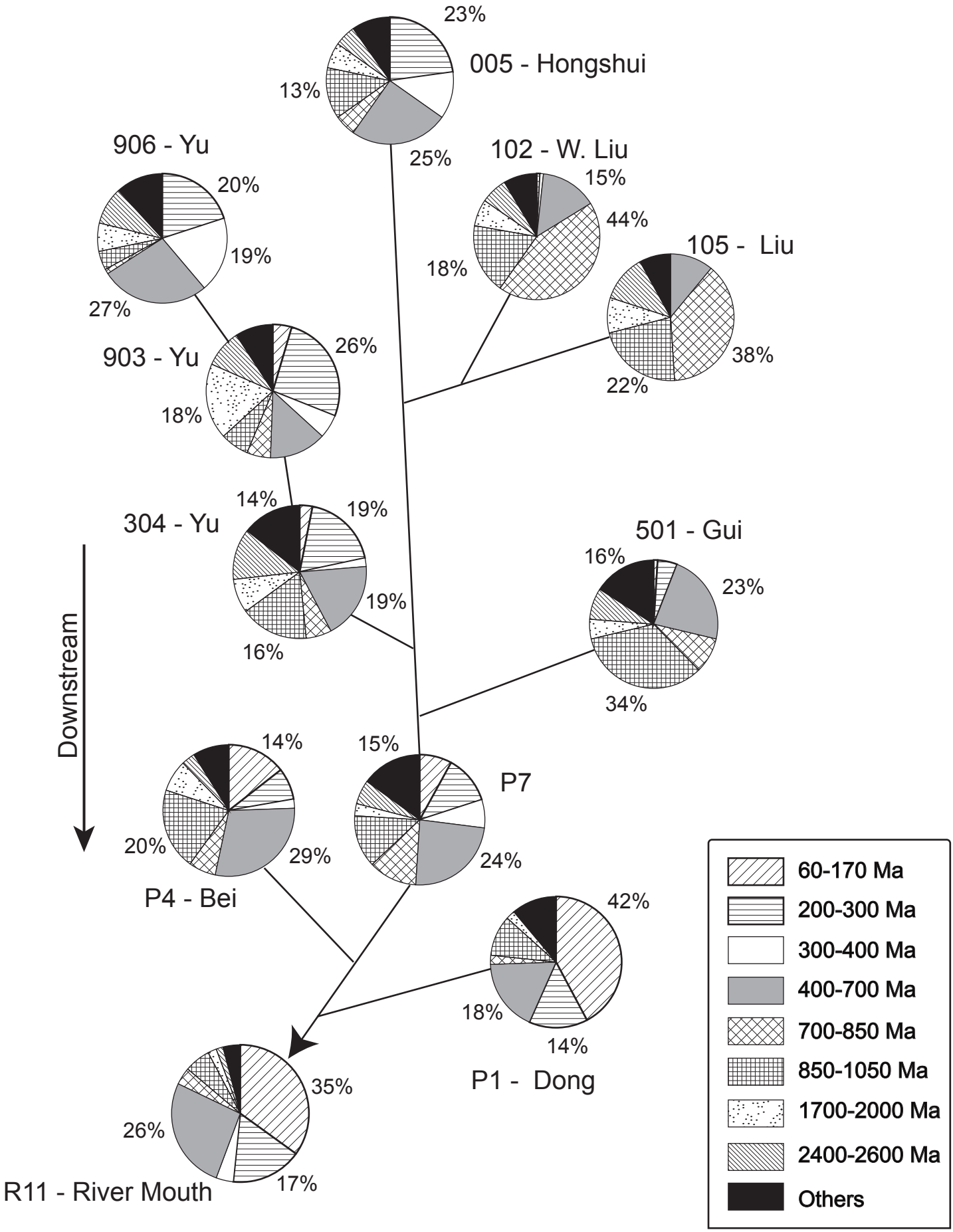

Figure 11
Liu et al.

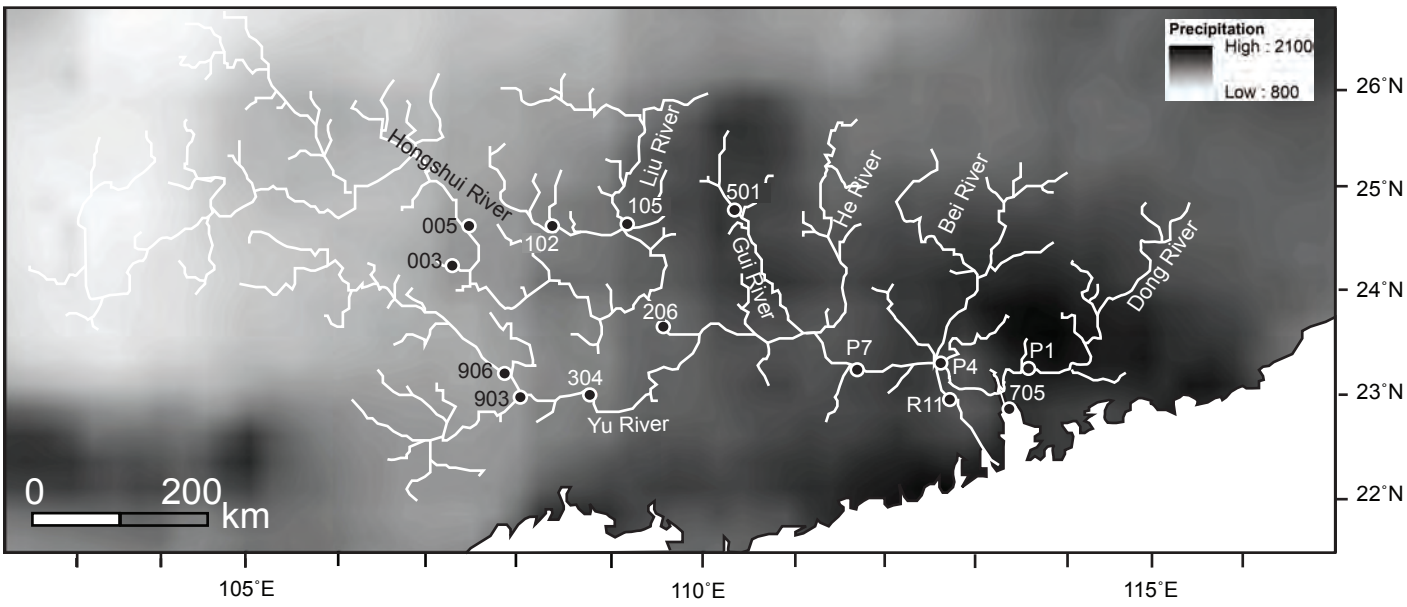

Figure 12
Liu et al